THE UNIVERSITY OF TEXAS AT AUSTIN
CENTER FOR TRANSPORTATION RESEARCH

TECHNICAL REPORT 5-6925-01-1
TxDOT PROJECT NUMBER 5-6925-01

IMPLEMENTATION OF IMPROVED PERFORMANCE GRADE (PG) OF ASPHALT BINDERS

Angelo Filonzi
Kiran Mohanraj
Manuel Trevino
Darren Hazlett
Amit Bhasin

June 2022; Published August 2022

http://library.ctr.utexas.edu/ctr-publications/5-6925-01-1.pdf

TECHNICAL REPORT DOCUMENTATION PAGE

1. Report No. FHWA/TX-22/5-6925-01-1	2. Government Accession No.	3. Recipient's Catalog No.
4. Title and Subtitle Implementation of Improved Performance Grade (PG) of Asphalt Binders Final Report		**5. Report Date** Submitted: April 2022 Published: August 2022
		6. Performing Organization Code
7. Author(s) Angelo Filonzi, Kiran Mohanraj, Manuel Trevino, Darren Hazlett http://orcid.org/0000-0002-8360-0022, Amit Bhasin https://orcid.org/0000-0001-8076-7719		**8. Performing Organization Report No.** 5-6925-01-1
9. Performing Organization Name and Address Center for Transportation Research The University of Texas at Austin 3925 W. Braker Lane, 4th Floor Austin, TX 78759		**10. Work Unit No.**
		11. Contract or Grant No. 5-6925-01
12. Sponsoring Agency Name and Address Texas Department of Transportation Research and Technology Implementation Division 125 E. 11th Street Austin, TX 78701		**13. Type of Report and Period Covered** Implementation Report September 2019–April 2022
		14. Sponsoring Agency Code

15. Supplementary Notes
Project performed in cooperation with the Texas Department of Transportation and the Federal Highway Administration.

16. Abstract
Given the importance of the quality of asphalt binder in resisting crack growth in asphalt mixtures, there is a critical need for a simple and accurate test to evaluate the cracking resistance of asphalt binders. Most current tests are based on rheological indices and do not induce cracking in asphalt binders. Researchers have developed a simple "poker chip" test to evaluate the cracking resistance of asphalt binders in terms of its ductility. The test method is simple, repeatable, sensitive, accurate, and does not require significant capital investment. This project demonstrated the sensitivity of the poker chip test to asphalt binder modifiers including polymers and chemical modifiers, polymer content, reclaimed asphalt pavement, and aging. This project also demonstrated that the test and resulting parameters are strongly related to the propensity of the asphalt pavement to crack. A study of 22 field sections from different geographic regions within Texas showed that 86% of field sections that had a ductility below 150% showed some form of cracking in the asphalt layer. This report presents the findings from this study as well as a standard method for adoption.

17. Key Words	18. Distribution Statement
Asphalt, Field studies, Thin films, Asphalt tests, Tension tests, Tensile strength, Ductility, Cracking, Fatigue cracking, Poker chip test	No restrictions. This document is available to the public through the National Technical Information Service, Alexandria, Virginia 22312, https://www.ntis.gov/.

19. Security Classif. (of this report)	20. Security Classif. (of this page)	21. No. of Pages	22. Price
Unclassified	Unclassified	121	

Form DOT F 1700.7 (8-72) Reproduction of completed page authorized

THE UNIVERSITY OF TEXAS AT AUSTIN
CENTER FOR TRANSPORTATION RESEARCH

Implementation of Improved Performance Grade (PG) of Asphalt Binders: Final Report

Angelo Filonzi
Kiran Mohanraj
Manuel Trevino
Darren Hazlett
Amit Bhasin

CTR Implementation Report:	5-6925-01-1
Report Date:	Submitted: April 2022
Project:	5-6925-01
Project Title:	Implementation of Improved Performance Grade (PG) of Asphalt Binders
Sponsoring Agency:	Texas Department of Transportation
Performing Agency:	Center for Transportation Research at The University of Texas at Austin

Project performed in cooperation with the Texas Department of Transportation and the Federal Highway Administration.

Center for Transportation Research
The University of Texas at Austin
3925 W. Braker Lane, 4th floor
Austin, TX 78759

http://ctr.utexas.edu/

DISCLAIMER

The contents of this report reflect the views of the authors, who are responsible for the facts and the accuracy of the information presented herein. The contents do not necessarily reflect the official view or policies of the Federal Highway Administration or the Texas Department of Transportation (TxDOT). This report does not constitute a standard, specification, or regulation. Mention of trade names or commercial products does not constitute endorsement or recommendations for use.

ACKNOWLEDGMENTS

The authors acknowledge the financial support of Texas Department of Transportation through Project 5-6925. The authors would like to acknowledge the support and help from the Project Monitoring Committee including Ryan Barborak, Enad Mahmoud, Roberto Trevino, Terry Sepulveda from The Materials and Tests Division (MTD) and Tom Schwerdt from the Research and Technology Implementation Division (RTI), in particular for providing access to the pavement performance monitoring database, which was developed as a part of TxDOT Project 0-6658 (Walubita et al., 2017). A special thanks to Darren Hazlett from The Center for Transportation Research (CTR) for his thoughtful input and help throughout the course of this project and to Tyler Seay from CTR for his work with binder lab testing and field coring from various locations throughout the state of Texas. Finally, the research team would also like to thank Bob Kluttz, Gary Fitts, and Sebastian Puchalski from Kraton Polymers for their help with polymer modification of some of the binders and to Scott Carroll from ADMET Inc. for his help with design of the load frame that can be used as a dedicated device to conduct this test.

ABSTRACT

Given the importance of the quality of asphalt binder in resisting crack growth in asphalt mixtures, there is a critical need for a simple and accurate test method to evaluate the cracking resistance of asphalt binders. Most current test methods are based on rheological indices and do not induce cracking in asphalt binders. As a part of a previous project, researchers identified the potential for developing and using a simple "poker chip" test to evaluate the cracking resistance of asphalt binders in terms of its ductility. This project further developed the poker chip test method to achieve a procedure that is simple, repeatable, sensitive, accurate, and would not require significant capital investment. This project also demonstrated the sensitivity of this method to asphalt binder modifiers including polymers and chemical modifiers, polymer content, reclaimed asphalt pavement, and aging. This project also demonstrated that the test and resulting parameters are strongly related to the propensity of the asphalt pavement to crack. A study of 22 field sections from different geographic regions within Texas showed that 86% of field sections that had a ductility below 150% showed some form of cracking in the asphalt layer. In some cases, reflective fatigue cracking and transverse cracking also showed a good trend with the measured ductility of the asphalt binders. This report presents the findings from this study as well as a standard method for adoption.

EXECUTIVE SUMMARY

There is a need to develop methods and concomitant parameters that can evaluate the full tensile behavior including non-linearity and damage resistance of asphalt binders. This need is underscored with the increasing use of asphalt binder modifiers, additives, and recycled materials. This study advances the findings from a previous study on the use of a poker chip test to evaluate the cracking resistance of asphalt binders.

During the first phase of this project, researchers focused on the development of a test procedure that was simple, repeatable, sensitive, accurate, and would not require a significant capital investment. To achieve a simple, easy and repeatable test specimen, researchers developed several prototype specimen holders to achieve a thin film that could then be subjected to a tensile strength test. The final version met these requirements by increasing the film thickness but also simultaneously increasing the diameter to achieve a similar degree of confinement.

The developed test method can be conducted using any generic universal testing machine that has a capacity of 5 kN or higher. However, in order to ensure that a dedicated equipment can be used for consistency across different locations, researchers worked with an equipment manufacturer, Admet, to develop a low cost loading frame that could be used to conduct this test. This device has a small footprint and does not require any special facilities beyond a 110V power supply.

In order to evaluate the sensitivity and qualitative accuracy of the test method, researchers used several different laboratory blended asphalt binders that have historically shown different degrees of performance in the field. In particular, researchers blended different base asphalt binders with different elastomeric polymers in different concentrations as well as other modifiers (e.g. a chemical modifier) that are typically not associated with improvements in cracking resistance. The results from these materials provide a very strong, albeit qualitative support to the proposed specimen fabrication and test method.

In order to benchmark the ability of the test method and ductility parameter to predict cracking in the field, researchers identified 22 field sections that were being monitored by Texas Department of Transportation (TxDOT) in another study (Walubita et al., 2017). Researchers obtained cores from these sections and used these cores to extract and recover asphalt binder samples. The ductility from the poker chip

test as well as other rheological properties were measured in this study. A comparison of field cracking to ductility indicated that 87% of sections that had a ductility of less than 150% also showed some form of cracking. It must be emphasized that these 22 sections were in very different climatic regions in the state of Texas and also varied in terms of mixture gradation, binder content, traffic volume, surface layer thickness and overall asphalt thickness. These results strongly support the ability of this test method to serve as a cracking indicator for an asphalt binder.

This report presents the findings from this study along with a standard test procedure that can be used on a routine basis to evaluate cracking resistance of asphalt binders.

TABLE OF CONTENTS

LIST OF FIGURES

LIST OF TABLES

CHAPTER 1. INTRODUCTION

The Performance Grading (PG) framework is currently used as the primary purchase specification and binder classification system in the state of Texas and many other parts of the world. Since its inception, binder production has evolved to include new technologies and additives to improve binder performance. However, in some cases such binders may also prematurely fail in asphalt pavements while still meeting the existing specifications. In light of this shortcoming, the research project 0-6925 reviewed various new methods that can be utilized as alternatives or in a complementary manner to the current specification.

A weakness in the current PG framework is the lack of a robust indicator for the inherent cracking resistance of asphalt binders at intermediate temperatures. Several researchers have explored a number of different approaches to evaluate the cracking resistance of asphalt binders. Most of these approaches can be classified into four broad categories: (i) time sweep tests typically conducted using a Dynamic Shear Rheometer (DSR), (ii) amplitude sweep tests also typically conducted using a DSR, (iii) measuring the ductility of the asphalt binder or a rheological surrogate for ductility, and (iv) measuring the strength of the binder in a realistic stress state (e.g. using thin films). The details on these categories, benefits, limitations, and accuracy of tests from each of the aforementioned categories can be found in Hajj and Bhasin (2018). One of the outcomes from the 0-6925 project was the strong correlation between laboratory measured fatigue cracking resistance of asphalt mixtures and cracking resistance of asphalt binders measured using a cohesion or poker chip test, which falls in the last of the four aforementioned categories. The main goals of this implementation project were to (i) refine this test method so it could be implemented and used on a routine basis, (ii) establish tentative specification limits based on field data for binder that may be susceptible to premature cracking, and (iii) facilitate training and technology transfer to TxDOT so laboratory personnel could perform this test on asphalt binders.

Chapter 2 of this interim report presents the field sections that were identified and selected to compare the results from the poker chip test with the results from the field. In addition to the field mixes, this study also evaluated the sensitivity and repeatability

of the test method using specially formulated laboratory mixes. A description of these materials is also provided in Chapter 2.

Chapter 3 presents a description of the various fixtures that were attempted to further refine and make the sample preparation and test method more repeatable. Some changes to the test protocol were also made to achieve the higher sensitivity from the test results.

Chapters 4 and 5 present the results from this study.

Appendix A presents a detailed step-by-step sample preparation procedure. Appendix B presents photographs from various pavement sections along with measures of ductility. Appendices C and D present the present of the procedure in standard TxDOT and AASHTO format. An instructional video with other details can also be found at https://doi.org/10.18738/T8/KTCNVK.

CHAPTER 2. MATERIALS, TESTS, AND PARAMETERS

2.1 MATERIALS FROM FIELD SECTIONS

2.1.1 Selection of field sites

As a part of a different study by Walubita et al. (2017), TxDOT developed a pavement performance database that documents the detailed properties of materials used during construction, characteristics of the pavement structure, and an yearly assessment of the performance of these pavement sections. This database was used to identify 22 field sections that had been in place for six years or longer.

Figure 2.1 shows the locations of the 22 field sections that were selected and evaluated in this study. Table 2.1 provides detailed information on these sections. Five different criteria were used to select these field sections: (i) construction date, (ii) climatic region, (iii) traffic condition, and differences in performance such as (iv) fatigue and/or (v) thermal cracking that can be attributed to the changes in the properties of the asphalt binder.

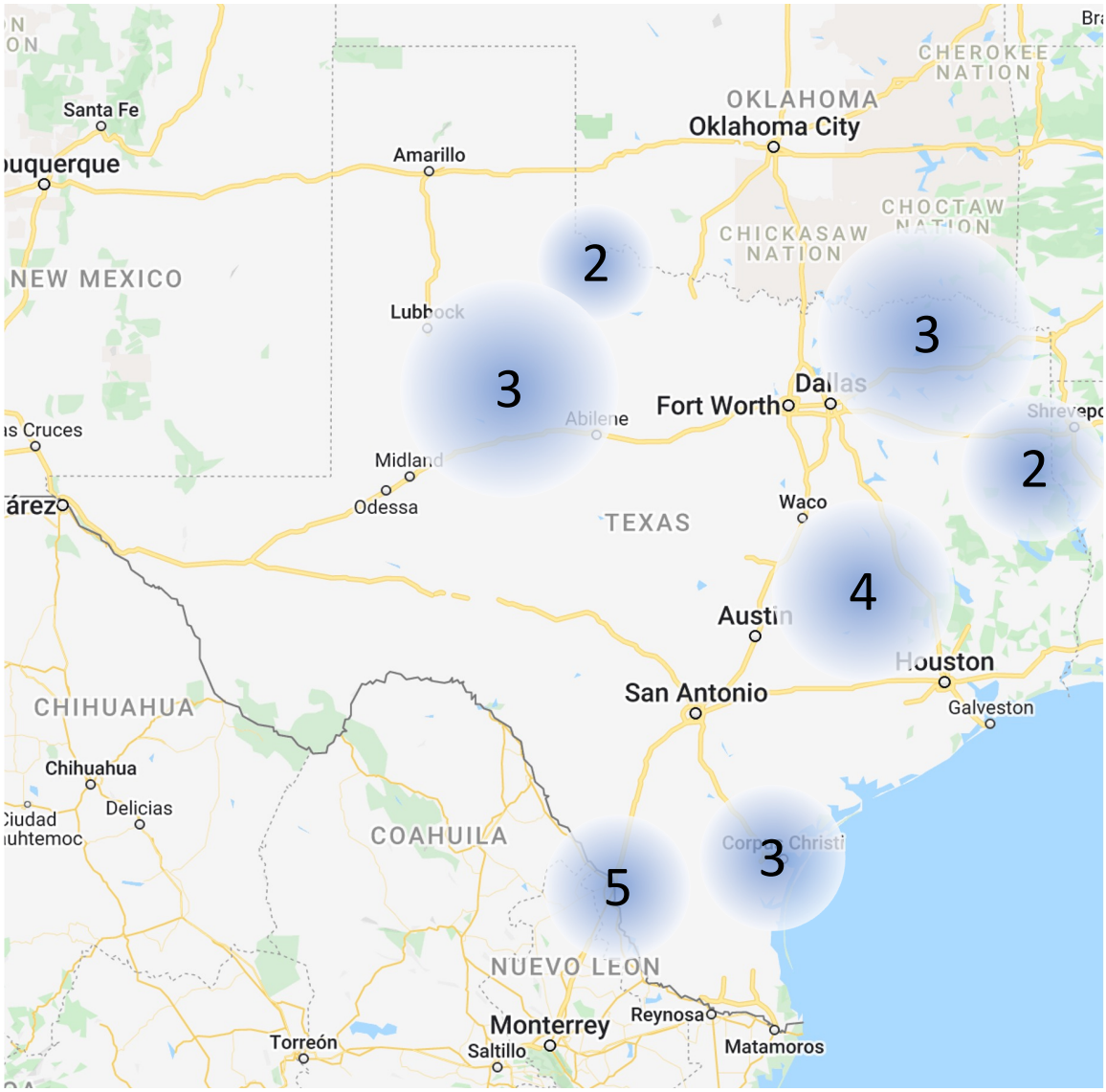

Figure 2.1. Locations of field sections selected for validation (Map Data: ©2021 Google).

Table 2.1. Details of field sections used in this study Walubita et al. (2017)

Section	Construction Year	Last Inspection Year	Total ESALs (million)	Total HMA Thickness (inch)	HMA Surface Course Thickness (inch)	Asphalt Content (%)	Design Asphalt Performance Grade	Fatigue Cracking, %	Transverse Cracking (cracks / 100ft)	Transverse Crack Spacing (feet)	Reflective Cracking (cracks / 100ft)
1	2011	2018	3.7	13.5	2	5.1%	64-22	15.0%	3	42	2
2	2011	2019	1.1	8	1.5	6.7%	76-22	0.0%	9	12	6
3	2012	2019	2.8	10	1.5	6.7%	76-22	0.0%	2	39	1
4	2012	2018	1.0	8.5	2	4.9%	70-22	2.9%	4	29	3
5	2014	2019	0.7	3.5	2	4.9%	64-22	0.0%	0	0	0
6	2012	2019	0.1	9.5	1.5	5.3%	64-22	0.0%	0	0	0
7	2012	2019	1.8	8.5	2	4.8%	64-22	0.0%	0	0	0
8	2012	2019	2.2	7.5	2.5	4.9%	64-22	0.0%	2	31	0
9	2010	2019	0.9	13	1	4.8%	76-22	0.0%	5	18	1
10	2012	2019	1.1	8	3	4.8%	64-22	0.0%	1	80	1
11	2010	2019	1.5	12	2	4.8%	64-22	0.0%	2	48	1
12	2010	2019	0.3	7	2	4.8%	64-22	4.7%	3	33	1
13	2014	2018	0.5	6	2	6.7%	76-22	0.0%	0	0	0
14	2010	2018	3.1	4.75	1.75	5.2%	64-22	0.0%	0	0	0
15	2014	2018	1.0	9.5	2	5.4%	64-22	0.0%	2	59	2
16	2010	2014	2.5	N/A	N/A	4.8%	64-22	0.0%	0	0	0
17	2012	2018	0.5	8.5	2	5.1%	64-22	9.6%	1	100	0
18	2011	2018	2.9	11.5	1	8.5%	58-22	0.0%	1	100	0
19	2011	2018	5.0	8	2	5.4%	70-28	1.3%	15	7	5
20	2012	2018	1.5	2	2	6.3%	70-28	1.7%	0	0	0
21	2012	2018	1.0	5	2	5.6%	70-22	0.0%	6	19	0
22	2012	2018	4.0	N/A	N/A	N/A	N/A	0.0%	1	100	0

Note 1: N/A indicates that the data were not available

Note 2: Total ESALs were computed using a growth rate of 1 to 2% depending on the section being considered and baseline data from the year of construction

2.1.2 Field coring and sample handling

Field cores (6-inch diameter) were obtained from each of the 22 field sections, with 4 to 8 samples obtained at each location. In sections experiencing fatigue and/or thermal cracking, 2 samples were located right next to the crack(s), and the other 6 samples were located further away from the distressed portions of the pavement sections. The coring and patching operations performed to obtain the field cores are shown in Figure 2.2. The field cores were carefully transported to the laboratory for further processing such as cleaning, photographic documentation, and storage, as shown in Figure 2.3 as an example of 8 field cores extracted from one of the field sections. The TxDOT pavement performance database also provides information related to the pavement layers thicknesses and material types. This information is key to identify the top layer thickness of each section considered for evaluation. The top layer of each core was cut/trimmed to avoid contamination from any remaining material related to the tack coat or lower layers, which might affect the binder properties and results of the tests performed after the extraction and recovery process. As an example, Figure 2.4 shows the top layer of field cores, after being cut using a wet-saw, for one of the field sections.

In some of the sections, the original asphalt layer under evaluation had been overlaid with a chip seal or a thin overlay as part of routine maintenance activities or pavement preservation projects. For such cases, the surface layer was saw-cut and discarded, and only the HMA layer corresponding to the measured field performance was used for further testing. All processed field cores were stored at 4°C (to retard aging) prior to being used for extraction and recovery of the asphalt binder.

Figure 2.2. Field coring and patching.

Figure 2.3. Field core samples.

Figure 2.4. Top layer of field core samples.

2.1.3 Extraction and Recovery of Asphalt Binder

Asphalt binder samples were obtained using conventional solvent extraction and recovery on all the processed cores including those collected from locations right next to cracks.

Figure 2.5 shows a centrifuge extractor that was used with toluene as the solvent to extract the asphalt binder from a sample of the loose asphalt mixture. The rotary evaporator method was used to recover the asphalt binder from the solvent following the method described in AASHTO TP2 (1999). Recognizing that toluene is a toxic solvent, as a safety measure, both the solvent extractions using the centrifuge extractor and the recovery using the rotary evaporator were performed under a fume hood. The extraction and recovery of all the cores for each location yielded approximately 40 g of asphalt binder. The following is a summary of the steps used for extraction:

1. A sample of loose HMA (1000 g) was obtained from heating the processed cores. Cores with visible contamination, primarily tack coat sticking to the sides of the core during the coring process, were trimmed off from the heated core (using a hot spatula) and discarded. The sample of this loose HMA was placed in the centrifuge bowl for extraction.
2. The centrifuge bowl was charged with 600 mL of toluene measured in a beaker. The bowl was carefully stirred ensuring no solution or material spilled from the bowl and the solvent thoroughly covered all of the material inside the bowl. The centrifuge was properly closed and set aside for one-hour to allow the solvent to fully soak all material.
3. The lid of the centrifuge bowl was removed, the loose asphalt-aggregate-toluene mixture was stirred, and a 4.0 μm paper filter was placed over the bowl followed by the lid (tightened). The centrifuge lid was then closed to ensure a tight seal.
4. The centrifuge was turned on until the solution stopped pouring out into the collection jar. At the end of extraction process, a lid was placed on the jar to seal the asphalt-toluene solution.
5. Steps 2, 3, and 4 were repeated until the solvent from the centrifuge was clear and all binder appeared to be extracted from the aggregates, based on visual examination.

The asphalt-toluene solution obtained was then transferred to the rotary evapo-

rator (shown in Figure 2.6) to recover the asphalt binder. The process summarized below for recovery of asphalt using the rotary evaporator (also known as RotoVap) was developed after conducting several trials asphalt binder with known properties extracted from loose asphalt mixture.

1. The oil bath was set to 80°C and allowed to reach the temperature.
2. Using a funnel, 500 mL of the binder-toluene solution was poured into a rotary evaporator round-bottom flask, and the flask was placed onto the lip of the rotary evaporator.
3. Cold water was circulated through the rotary evaporator and all vacuum release valves were closed and the vacuum pump was turned on to reach a vacuum of at least 65 cm Hg.
4. The rotary evaporator was lowered to a height that ensured the solution-line on the round-bottom flask was fully submerged in the oil bath while rotating.
5. The temperature was raised over time to maintain a visible flow of toluene, and then to a maximum temperature of 165°C.
6. When there was no more visible trace of toluene inside the flask, the flask was raised out of the oil bath, the vacuum pump was turned off, the vacuum was released, and the remaining recovered asphalt binder removed out of the flask into a metal container.

Figure 2.5. Centrifuge extractor used with toluene as the solvent to recover the asphalt binder.

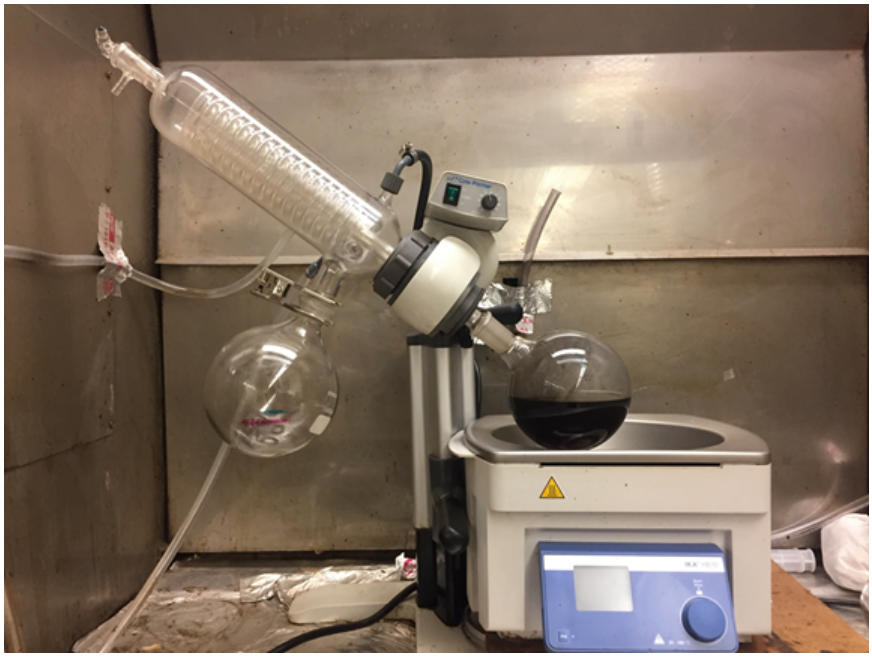

Figure 2.6. Rotary evaporator used to recover the asphalt binder.

2.2 LABORATORY FORMULATED AND PRODUCER SUPPLIED PERFORMANCE GRADE BINDERS

In addition to the field validation, it was also important to assess the results obtained from the test method using asphalt binders that were specially formulated in the laboratory and binders commercially supplied by various producers. In the context of this study, these binders can be categorized into the following groups.

- Group 1: The binders in this group were used to assess the differences in the material response based on their performance grade (PG). This group included PG 58-28 (4 samples), 64-22 (32 samples), 64-28 (4 samples), 70-22 (39 samples), 70-28 (8 samples), 76-22 (37 samples) and 76-28 (6 samples). The aforementioned binder samples were obtained from different producers and in some cases also include multiple samples from the same producer but sampled at different points in time. All binders in this group were evaluated after Rolling Thin-Film Oven (RTFO) and Pressurized Aging Vessel (PAV) aging. This group had a total of 130 binders that were evaluated in two different aging conditions.
- Group 2: The binders in this group were used to assess the impact of an elastomeric polymer on the measured parameters. The evaluation included three base binders from different sources that were blended with three different percentages (1.5, 3.0, and 4.5%) of a commonly used elastomeric polymer. The blends were evaluated after RTFO and PAV aging the binders, resulting in a total of 12 binders including the control. These 12 binders were evaluated in two different aging conditions.
- Group 3: The binders in this group were used to assess the impact of a chemical modifier that is sometimes used to enhance the high temperature grade of an asphalt binder. The evaluation included two base binders from different sources that were blended with 1.5% of the chemical modifier. The binders were evaluated after both RTFO and PAV aging, resulting in a total of 8 binders including the control and the two aging conditions.
- Group 4: The binders in this group were used to assess the impact of a another common industrial waste product that is used as a modifier for asphalt binders. The evaluation included four base binders from different sources. Two of these binders were blended with 5.0% of the modifier and the other two binders were

modified using 2.5, 5.0, and 7.5% of the modifier. These binders were evaluated only after RTFO aging, resulting in a total of 12 binders.

2.3 TEST METHODS AND PARAMETERS

Some early field studies performed by Clark (1958) found that there was a complete lack of ductility in the thin films of binder in the sections analyzed as "failed" pavements. Clark (1958) also reported that the pavements analyzed to be "good" sections had high ductility and vice-versa. He proposed ductility as a preferred parameter over penetration that measured embrittlement due to aging of asphalt binder, which may be considered as a predictor for fatigue cracking in field aged samples. The same year, Doyle (1958) performed a field study using five different asphalt binders placed at two different locations in Ohio. They measured the ductility of binders extracted from field cores of sections in service for at least five years. Sections where cracking was observed had low ductility values of 3 and 4, while the section with no cracks had a ductility value of 29. The study also found that ductility measured at 55°F at a test rate of 1 cm per minute or lower correlated well with results seen in the field sections. The study concluded by suggesting the use of ductility to predict cracking by testing both original and aged asphalt binders. Several subsequent studies have emphasized the importance of ductility of the asphalt binder as an indicator for cracking resistance (Halstead, 1962; Heukelom, 1966; Kandhal, 1977; Kandhal and Koehler, 1987).

Interestingly, the concept of loss in ductility at low and intermediate temperatures was not incorporated in the PG framework that followed the aforementioned studies. Furthermore, the study by Glover et al. (2005) was motivated by some of the aforementioned studies to find a surrogate parameter for ductility that can be measured in the laboratory using a DSR, which had become the cornerstone instrument following the development of the PG framework. This led Glover et al. (2005) to approximate the behavior of the binder using a Maxwell model and propose the parameter $G'/(\eta'/G')$ as a surrogate for ductility.

More recently, Rowe et al. (2014) evaluated three different pavement sections as part of a case study performed on an airport in the northeast US. The three sections included two polymer modified (SBS) binders and one PG 64-22 binder. The primary concern that triggered the study was reported as accelerated oxidation and raveling of the polymer modified asphalt binder surfaces. Based on the results, it is

reported that polymer modified asphalt binder aged faster than PG 64-22, and that the binder stiffness at intermediate temperatures did not appear to explain the surface damage. The analysis was performed using the $G^*(\cos\delta)^2/\sin\delta$ parameter, which is the parameter from Glover et al. (2005) in a different form and at a constant angular frequency ω. The parameter, also referred to as the G-R parameter, was found to correctly predict initiation of damage for both modified binders in terms of raveling and approaching the zone where it can start to exhibit surface cracking, whereas the conventional asphalt showed little aging. The authors also evaluated the three sections using another parameter referred to as the *R-value* and found it to be an ineffective parameter in predicting aging related damage.

Bennert et al. (2017) studied five runways that were part of Port Authority of New York and New Jersey (PANYNJ), each of which consisted of a different asphalt overlay, placed at different times, and representative of a different level of field cracking performance. Their research study evaluated 2-inch thick field cores where the top 0.5-inch and bottom 1.5-inch portions were separated, extracted and tested. Comparative analysis of these separated portions included determination of ΔT_c and G-R parameters. In contrast to the previous study, they reported that ΔT_c appeared to provide a better indication of cracking observed in the field sections compared to the G-R parameter. The information from the study was further used to justify incorporating ΔT_c in purchase specifications to minimize premature top-down fatigue cracking due to accelerated aging.

One of the characteristics of the aforementioned studies from Accelerated Loading Facility (ALF) or the airfield pavements was that the different sections within each study were built with very similar material characteristics (other than the asphalt binder), and subjected to similar traffic and environmental conditions. Consequently the comparisons and concomitant conclusions were validated within each group of sections. This also explains the discrepancy in the results reported for similar parameters by Glover et al. (2005) and Bennert et al. (2017). Finally, two other more recent studies are summarized below.

Zhang et al. (2021) evaluated relationships between laboratory and field measured transverse and fatigue cracking on 23 pavement sections and statistically developed parameters for both cracking types. The laboratory binder testing did not include any of the aforementioned parameters (e.g. G-R or R-value) but included the temperature

and frequency sweep test and the monotonic stress-strain sweep test at intermediate and low temperature. Mixtures were evaluated for their complex modulus (E^*), and the indirect tensile strength at intermediate and low temperatures. Based on the results of the statistical analysis (Pearson Correlation Coefficient and Spearman Rank Correlation Coefficient) of various parameters, a preliminary thermal cracking threshold was proposed as a function of asphalt binder content and binder failure strain (as determined by Monotonic Sweep Test).

More recently, Christensen and Tran (2022) evaluated asphalt binder properties that are significant indicators of the fatigue performance of asphalt mixtures. The study evaluates various rheological parameters of asphalt binders including G-R parameter and R-Value, and their correlations with fatigue cracking performance in both laboratory and field. Three sets of pavements were considered located in Arizona, Minnesota, and Alabama (NCAT test track) with each set consisting of four test sections. Asphalt binders from the National Center for Asphalt Technology (NCAT) test track were recovered at NCAT and provided to the researchers for further testing. The study reports poor to good correlation with $|G^*|\sin\delta$, and moderate to good correlation for the G-R parameter and $|G^*|(R/2)^2$. However, it is important to emphasize that these correlations were developed for each set of sections separately even though the test temperature for the parameters were adjusted based on average pavement temperature. The study also included a second set of validation with similar results using data from five sections from the Federal Highway Administration's Accelerated Loading Facility (FHWA ALF) fatigue experiment.

Based on the aforementioned studies, the following three parameters were considered for evaluation:

1. Ductility as measured using the poker chip test (a detailed test procedure is included at the end of this report in an Appendix).
2. The Glover-Rowe parameter measured using the 8 mm diameter parallel plate geometry.
3. The ΔT_c parameter measured using the Stiffness (S) and m-value. In this study, these values were obtained using the 4 mm diameter parallel plate geometry with a Dynamic Shear Rheometer.

CHAPTER 3. DEVELOPMENT OF SPECIMEN FABRICATION AND TEST PROCEDURE

3.1 BASIC RHEOLOGICAL PROPERTIES OF THE ASPHALT BINDERS

The binders identified in Chapter 2 were evaluated for their basic rheological properties. These rheological properties were intended to serve as a baseline to compare binder properties. In the case of binders obtained from field cores, the properties were measured on the recovered binder on "as-is" basis, i.e. no additional aging or conditioning was carried out on the extracted binder. In the case of laboratory formulated binders, the properties were measured using unaged, short-term aged, and long-term aged binders as appropriate for any given metric. The poker chip test was carried out using only short-term aged and long-term aged binder samples. The following methods and metrics were evaluated for the binders extracted from the field cores.

1. Continuous high grade using 25 mm parallel plate geometry with a Dynamic Shear Rheometer (DSR)
2. Non-recoverable creep compliance (J_{nr}) using 25 mm parallel plate geometry with a DSR following the multiple stress creep and recovery (MSCR) test protocol
3. Elastic recovery using 25 mm parallel plate geometry with a DSR following the multiple stress creep and recovery (MSCR) test protocol
4. Continuous low temperature grade and ΔT_c using a Bending Beam Rheometer (BBR) and
5. Continuous low temperature grade and ΔT_c using 4 mm parallel plate geometry with a DSR
6. Glover-Rowe parameter using 8 mm parallel plate geometry with a DSR

3.2 REFINEMENT OF THE POKER CHIP SAMPLE PREPARATION METHOD

3.2.1 Preliminary designs for specimen fabrication

The preliminary work done in the 6925 project involved using a poker chip test specimen that was 350 μm thick confined between cylindrical pegs that were 10 mm in diameter.

The thin film specimens were prepared using an Instron loading frame or a Dynamic Shear Rheometer (DSR). In summary, the top peg of the poker chip specimen was attached to the top part of the frame and the lower peg to the lower part of the frame. The top cross head of the frame was then lowered until a small normal compressive force was detected and the position of the frame. This point was recorded as the zero gap. The top cross head was then raised and the faces of the poker chip pegs were heated using a small butane burner. A sample of the binder was then placed on the bottom face and the top cross head was lowered to achieve approximately 500 μm film thickness. The excess binder was then trimmed from the sides and the top cross head was further lowered to achieve the target film thickness of 350 μm. The binder was allowed to relax for 15 minutes at the target test temperature. The loading frame was adjusted to relieve any excess tensile stress developed due to the contraction of the binder as it cools down. The final gap before conducting the test was also recorded to compute the strain.

The research team realized that it required significant skill and training to be able to prepare test specimens in this manner to obtain in repeatable test results. Also, the lack of temperature control to condition the specimen and the plates at the time of specimen preparation and the movement of actuator to achieve the target film thickness would contribute to the variability. On account of these challenges, researchers investigated a different approach to prepare and test the thin film specimen. The following is a brief summary of some of these specimen fabrication methods.

The first attempt was to develop a process that did not rely on the test equipment itself to create the test specimen. This is an important factor because it ensures that the testing time on the instrument is significantly reduced and multiple samples can be fabricated and tested on a production scale. Figure 3.1 shows the jig that was fabricated and attempted for use with this philosophy. The goal was to heat the metal plates and use silicone blocks as a spacer to control the film thickness and also could be easily removed after the sample was prepared. A notable departure was the use of a square testing face instead of a circular geometry. This would introduce stress concentrations and edge effects but would fundamentally retain the main attributes of the test. However, it was observed that in practice, a significant compressive pressure was required to ensure that the film retained its position as it cooled. It was not feasible to ensure a consistent amount of pressure from one replicate to another. As

a result, this iteration was not pursued any further.

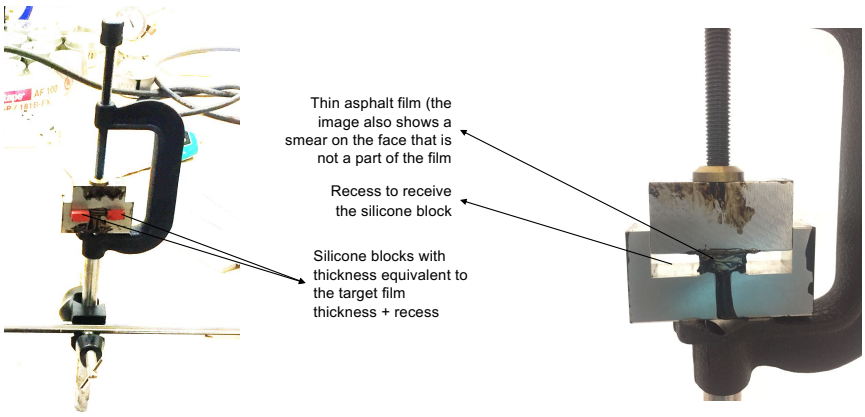

Figure 3.1. The first iteration using silicone blocks as spacers to prepare thin film specimens.

In order to improve the above version, the silicone blocks were removed and a three piece system was designed. The three piece system had two slotted plates that comprise the test geometry and a base plate with machined pegs that were spaced so that when the slotted plates were pressed towards each other the gap created would be the desired film thickness. Figure 3.2 shows the design of this fixture along with the fabricated parts and a sample. This variation also used a square cross section, similar to the previous iteration. This approach worked adequately. However, it was deemed as not practical in the future for the following reason. The target film thickness was being achieved by machining pegs in a block and slotted sample holders. This requires special high tolerance machining that is accurate to $\pm 0.001''$ or $\pm 2.5\mu m$ instead of conventional machining that is accurate to $\pm 0.005''$ or $\pm 12.5\mu m$. Even with a tolerance of $\pm 0.001''$ or $\pm 2.5\mu m$ in individual component, the compounded error between the parts could be has high as four times this value, i.e. $\pm 0.004''$ or $\pm 10\mu m$, which would result in a 3% variability even before accounting for other factors that can further exacerbate the overall variability in test results.

Based on the previous two iterations, the geometry was reverted back to a circular cross section and several different procedures to prepare a thin film outside of the test equipment using a micrometer were attempted. Figures 3.3 and 3.4 show two different setups using micrometers that were used to cast thin films on the pegs used for testing. In one case a hot plate was used directly beneath the peg to maintain the

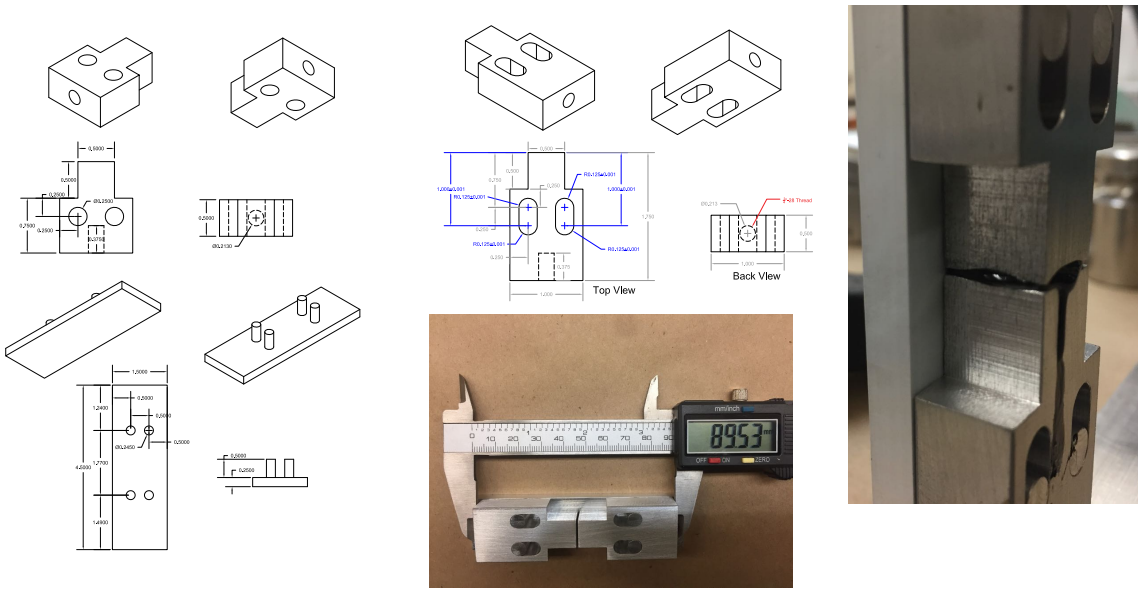

Figure 3.2. The second iteration using a metal base with pre-spaced pins and slotted plates to prepare the film.

temperature and facilitate casting of the thin film. Due to the height of the fixture, these attempts resulted in difficulties with the centering and vertical alignment of the top and bottom fixture. Small variations in the alignment with such a thin film would again result in variability in the test sample and the test results.

To alleviate this a 3D printed alignment frame (Figure 3.5) was also fabricated and evaluated. In addition, a dynamic shear rheometer (DSR) was also used to prepare such films (Figure 3.6). The use of a DSR resulted in films with excellent thickness control, temperature control, and alignment but then it also invalidated one of our core goals, i.e. to prepare the test specimen without the aid of any specific instrument.

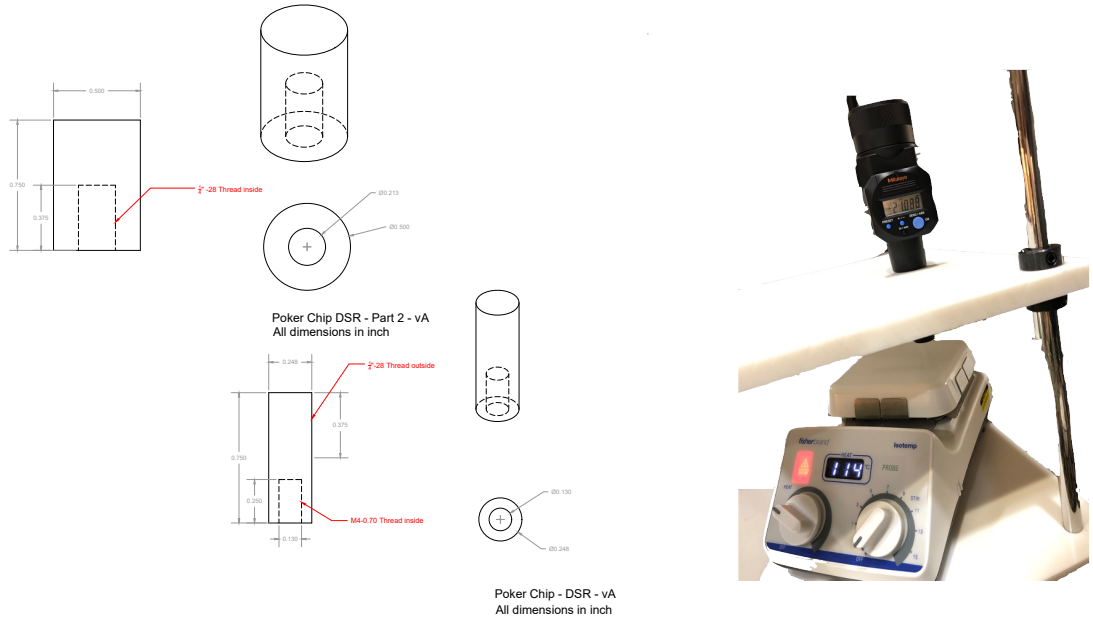

Figure 3.3. Third iteration of the sample preparation jig that utilized a micrometer with the top portion of the poker chip peg to achieve target film thickness while the bottom portion rested directly over a hot plate.

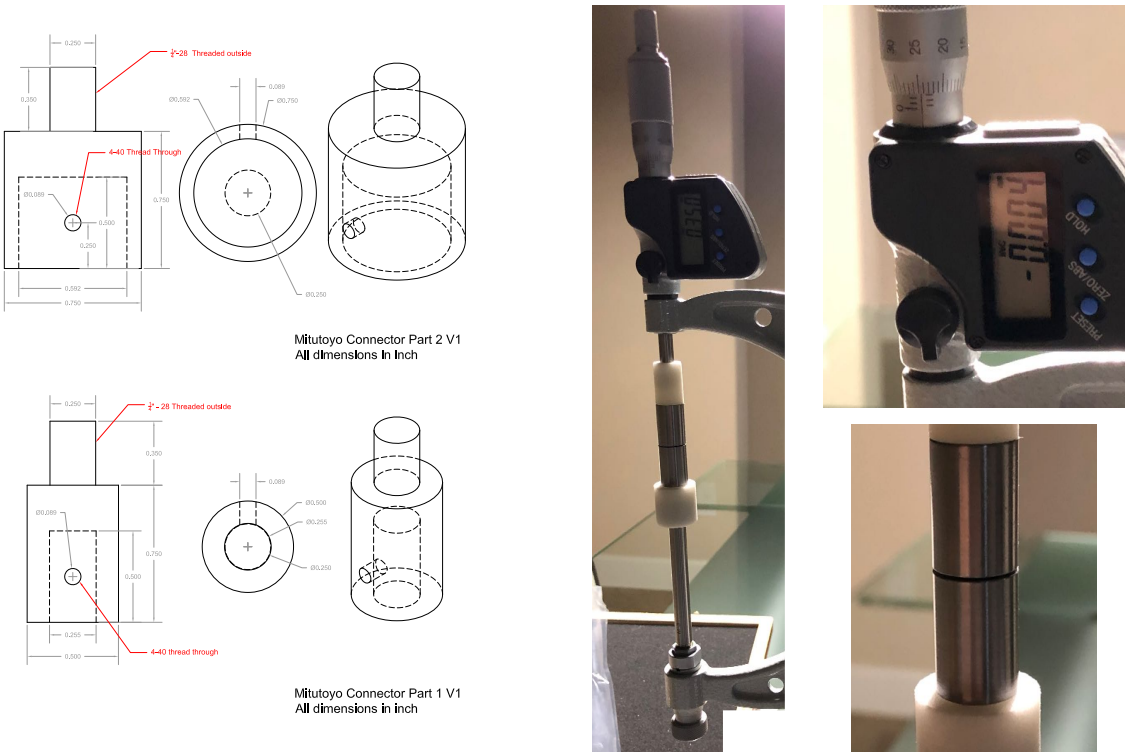

Figure 3.4. A variation of the third iteration with the top and bottom pegs affixed to a single frame micrometer but without the use of a hot plate; this iteration was intended to overcome the vertical alignment issues encountered with the previous iteration.

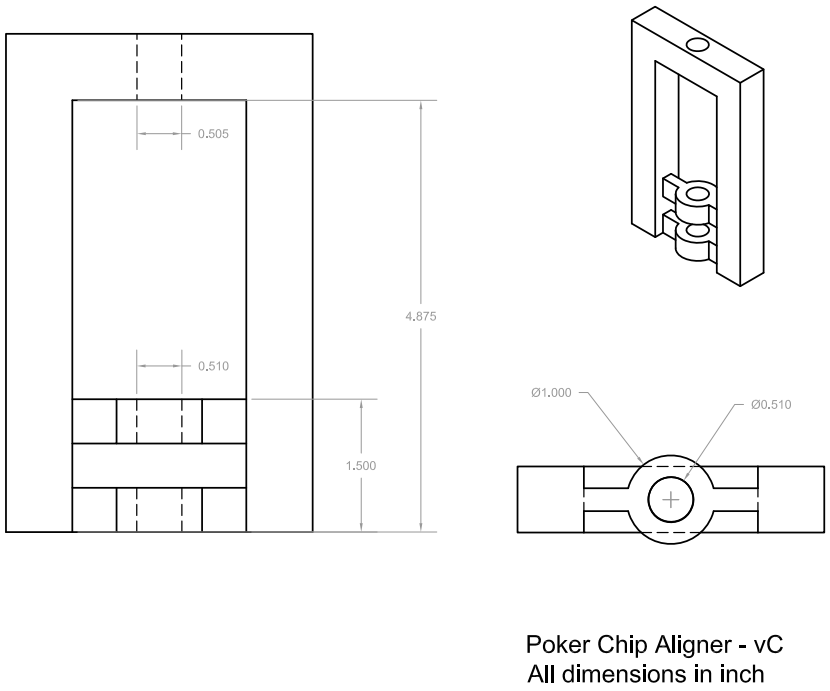

Figure 3.5. Fifth iteration that used a 3D printed frame to achieve vertical alignment with a micrometer on the top while allowing the use of a hot plate with the bottom peg.

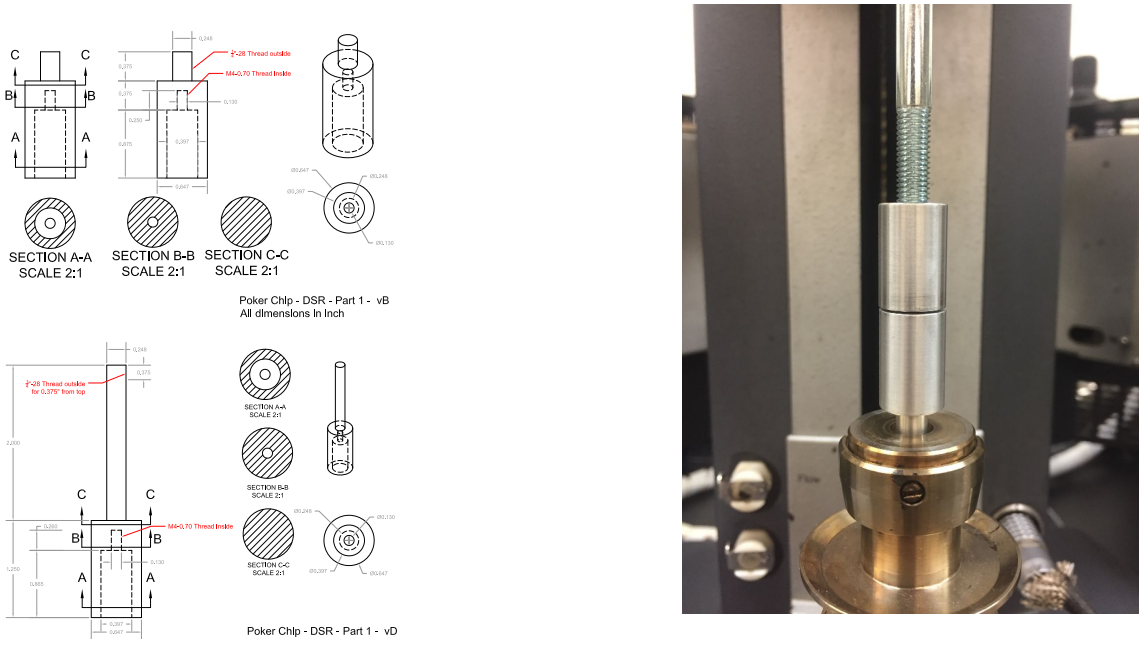

Figure 3.6. Sixth iteration that required the use of DSR to achieve temperature control, maintain alignment and precise film thickness in the sample.

3.2.2 Final design for specimen fabrication

All the aforementioned variations to prepare test specimens were designed to:

1. achieve a film thickness of 350 μm on a substrate that was approximately 10 mm in diameter,
2. ensure that the test fixture retained vertical and horizontal alignments to prevent eccentric loading during the test, and
3. be able to prepare the test specimens without the aid of a test equipment and in a manner that is easy to replicate in a typical lab setting by technicians performing the test.

Based on the experience in developing different methods to quickly and repeatably prepare test specimens, it was concluded that it may not be feasible to achieve all the above requirements simultaneously. The first requirement, i.e. a film thickness of 350 μm basically stems from a body of previous research that indicates that the asphalt binder film must be confined to achieve a state of stress that is a realistic representation of the state of stress in an asphalt mixture. To this end, previous studies (Sultana et al., 2014; Hajj and Bhasin, 2018) have shown that such a stress state can be achieved by maintaining an aspect ratio of approximately 30 or higher (ratio of diameter to film thickness). Keeping this basic tenant in mind, another alternative test geometry was explored by increasing the film thickness and corresponding increasing the diameter of the test specimen. Specifically, a 2-inch diameter test specimen was selected with a film thickness of 1/16-inch to provide an aspect ratio of 32. This configuration would require more binder sample but it would be significantly more tolerant to micron scale variations in the film thickness.

Figures 3.7 and 3.8 show the fabrication details for this test fixture. Another significant improvement that was made in the specimen fabrication process was the use of three small dowels embedded in the binder sample to control the film thickness. These dowels (McMaster-Carr Part Number: 98381A413) were $\frac{1}{8}$" ± 0.010 in length and $\frac{1}{16}$" $+0.0001$ to $+0.0003$ in diameter. The tight diameter tolerance creates an automatic "stop" point at the target film thickness when the top plate is placed over heated liquid asphalt binder without the aid of any external aid. Similar approach is employed using glass beads to prepare films for the T-peel test (Mohammed et al., 2016) and in bond tests with asphalt tack coats (Hazlett, 2020). The impact of a

discontinuity introduced from such a small intrusion on the overall test results (considering the now significantly larger diameter) is small compared to the benefits of achieving a simple and consistent sample fabrication procedure. Based on tests conducted using this geometry, the procedure was found to be extremely robust and viable for routine use. This procedure was then adopted for the remainder of the tests. Appendix C presents a detailed description of this test procedure in a standard TxDOT format and Appendix D in AASHTO format.

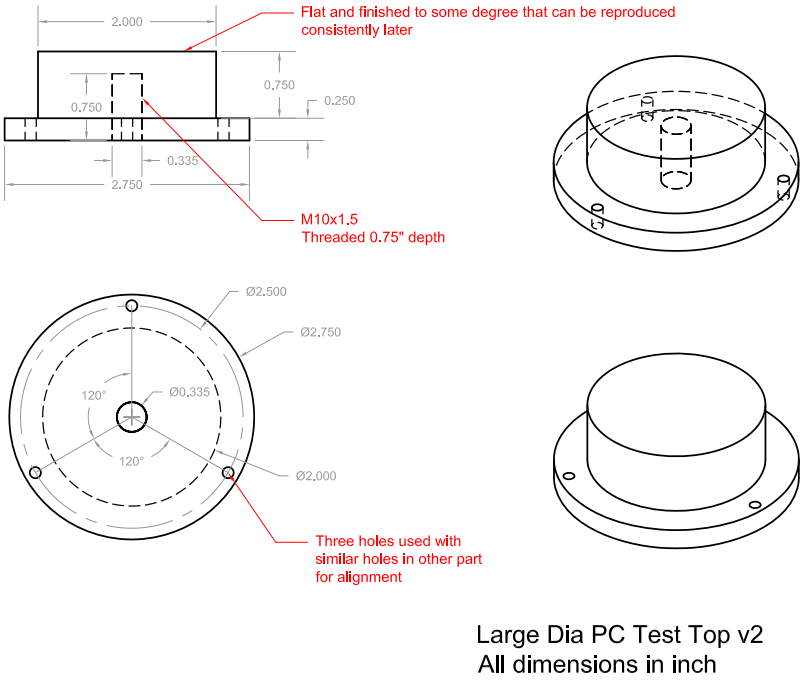

Figure 3.7. Final version of the top plate of the poker chip test.

3.3 POKER CHIP TEST METHOD

The cohesion test is carried out by applying a load that is increasing at a constant rate of 2 N/second. The load is applied until the specimen fails and during this time the load and displacement are recorded at a rate of at least 2 points per second. Figure 3.9 shows the typical applied load during the test and Figure 3.10 shows the typical stress-strain curve obtained from the test.

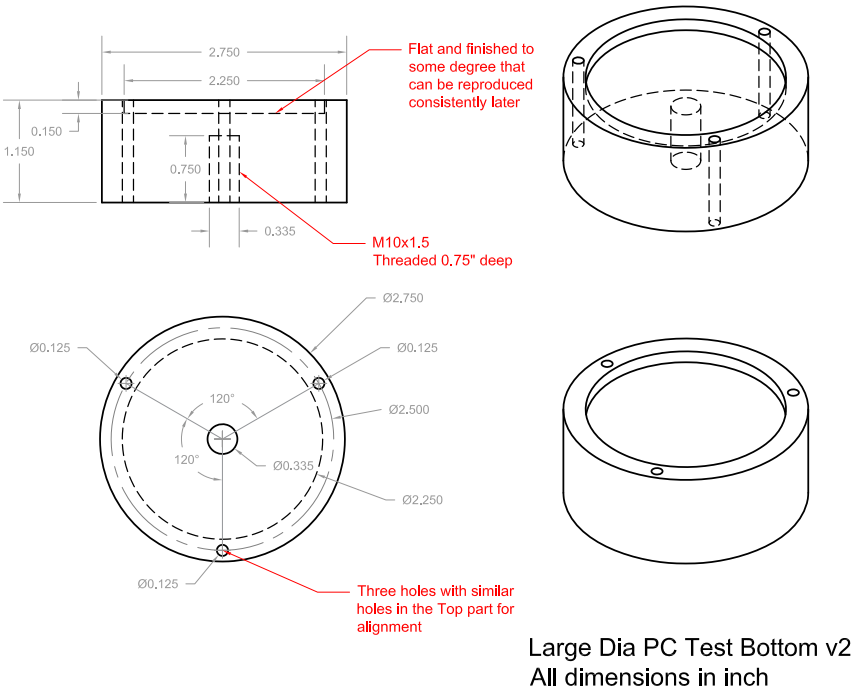

Figure 3.8. Final version of the bottom plate of the poker chip test.

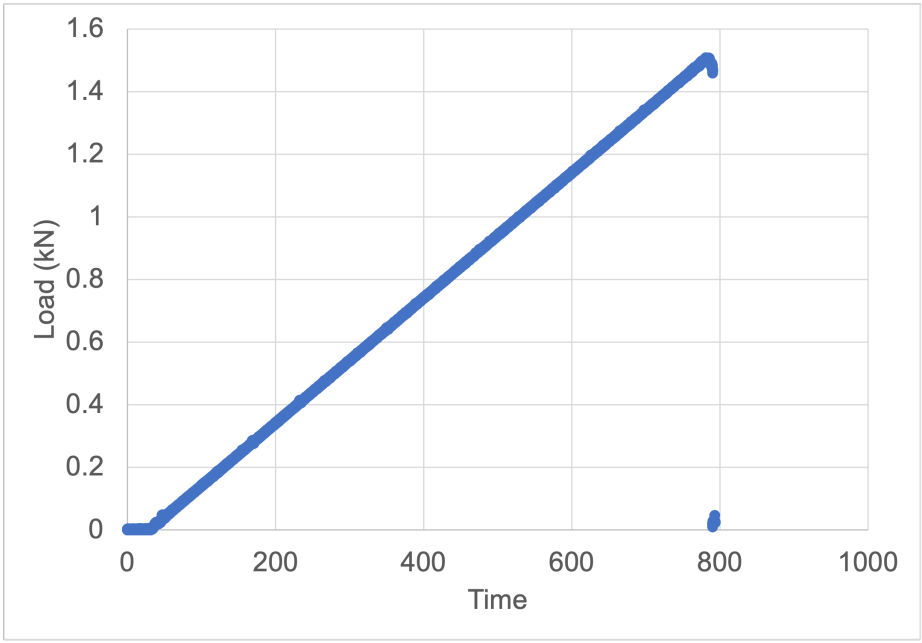

Figure 3.9. Typical load versus time applied during the test.

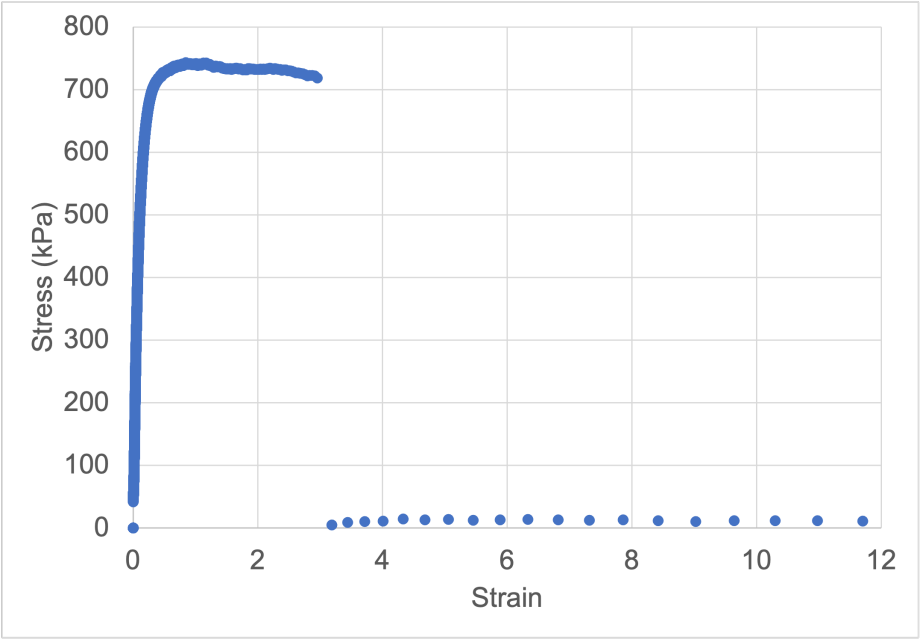

Figure 3.10. Typical stress versus strain curve recorded from the test.

CHAPTER 4. RESULTS FROM LABORATORY FORMULATED AND PRODUCER SUPPLIED PG BINDERS

This chapter presents the results from evaluating all the laboratory formulated and producer supplied performance grade (PG) binders identified in Chapter 2. The ductility results for each group are discussed in seriatim along with key findings from each group. The results for tensile strength are discussed at the end of this chapter.

4.1 REPEATABILITY

The results from 180 different binder tests were analyzed. These include binders with different levels of aging as well as binders extracted from field cores and reclaimed asphalt pavement (RAP) stockpiles.

The average coefficient of variation of these results was 9% with a standard deviation of 9%. The average coefficient of variation of tensile strength was 7% with a standard deviation of 5%. Also, all measurements were made using the same loading frame. Approximately 80% of the measurements were made by the same operator and the remaining by two other operators. A limited number of samples were tested by different individuals. Although a rigorous inter- and intra-laboratory study was beyond the scope of this work, preliminary results did not show substantial differences between operators.

4.2 GROUP 1 - DIFFERENCES IN DUCTILITY FOR DIFFERENT PG BINDERS

Figures 4.1 and 4.2 present the results for ductility measured using commercial PG binders after both RTFO and PAV aging. A few key observations from these results are:

- Ductility of PG58-28 and 64-22 binders appears to be similar after RTFO aging. Also, although there were only four PG58 binders from very different sources, the ductility values were similar for each grade (although this could change if additional binders from more diverse sources were added to the pool).
- Ductility of PG70-22 binders showed a marked increase compared to the ductility of PG64-22 binders. This is expected because PG70-22 binders are likely to be polymer modified using elastomers to meet the elastic recovery requirement per

the specifications in the state of Texas at the time of this writing. Also, the PG70-22 binders showed a larger diversity in the ductility values compared to the PG64-22 binders, possibly due to different amounts and/or types of polymer added to each binder.

- For the PG76-22 binders, the average ductility was interestingly similar to the PG70-22 binders, although the differences among the three different sources were much more pronounced. One of the PG76-22 binders had a very low ductility value (nearly 300%) compared to other PG76-22 and PG70-22 binders. Upon closer examination it was found that this binder had a continuous high grade of 82°C (even though it was being supplied as a PG76) which possibly resulted in higher elasticity at lower temperatures but not necessarily higher ductility as defined in the context of this study.
- The impact of PAV aging on ductility was clearly evident from the results. In all cases, as expected, the ductility reduced. However, a more interesting observation was that some binders were more resistant to aging than others, i.e. some binders retained higher ductility even after PAV aging compared to others. This will be discussed again in subsequent sections.

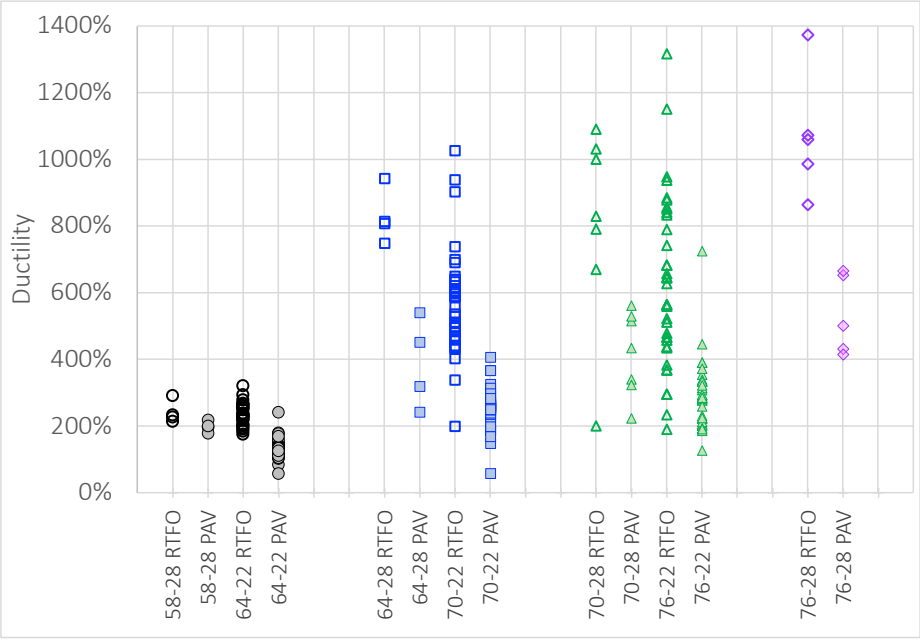

Figure 4.1. Range of ductility values measured for RTFO and PAV aged binders with different Performance Grades.

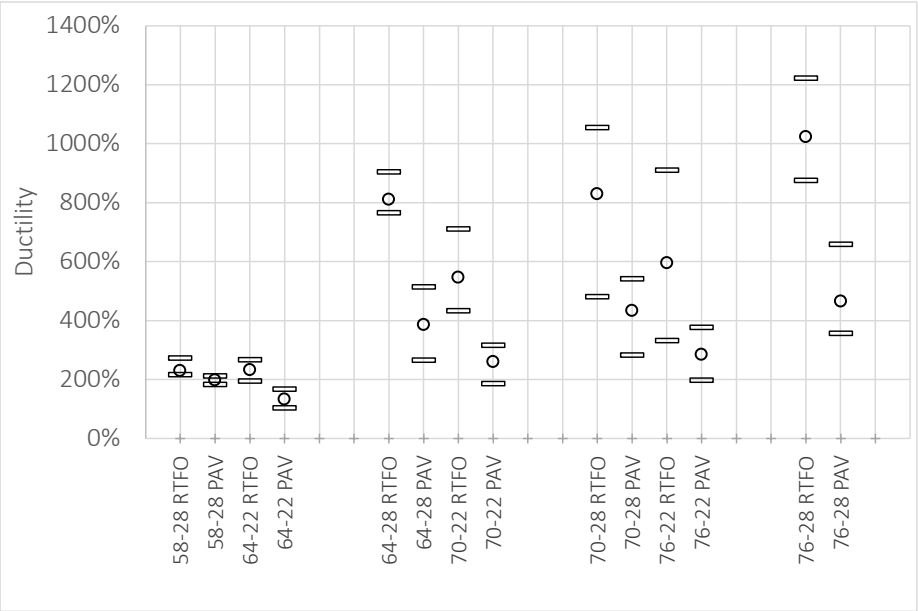

Figure 4.2. Median along with 10 and 90th percentile of ductility values measured for RTFO and PAV aged binders with different Performance Grades.

4.3 GROUPS 2, 3, 4 - IMPACT OF MODIFIERS

The asphalt binders evaluated in the previous sections were commercial PG binders, for which no information was available with regards to the modifier(s) used (if any) and the concentration of such modifiers. It was of interest to examine the impact of modifiers on the ductility parameter used in this study. To this end, binders in Groups 2, 3, and 4 were blended using a common elastomeric polymer (referred to as M1), a chemical modifier commonly used to enhance the high temperature grade of the binder (referred to as M2), and a third modifier that is also used as an extender with asphalt binders (referred to as M3). Figures 4.3 through 4.5 present the ductility of the base and the modified binders after both RTFO and PAV aging. The average ductility values from Group 1 for PG64 and PG70 grade binders (after RTFO aging only) are also included to provide a visual reference. Some of the key observations are as follows.

- Figure 4.3 clearly shows the increase in ductility of the binder with an increase in the elastomeric polymer concentration after RTFO aging. The three different base binders follow a slightly different trend but all three binders show this

increasing trend very clearly.

- Also from Figure 4.3, after PAV aging, the ductility for the binders with 1.5% elastomer was similar to the base binder. However, at higher concentrations (3 and 4.5%), the binders continued to show slightly increased ductility compared to the base binder even after PAV aging.
- Figure 4.4 shows that the chemical modifier M2 did not result in any increase in ductility compared to the base binder. In fact, the ductility appears to decrease slightly for both binders. Results after PAV aging also show no substantial difference between the base and the modified binder. This emphasizes the importance of moving beyond Performance Grading (PG) as the dominant method for classifying asphalt binders in the United States; although modifiers such as M2 can achieve similar benefits to elastomers in improving PG of a binder, they can ultimately prove ineffective in improving nonlinear binder properties in the same way, which is not captured by linear viscoelastic (LVE) indicators.
- Figure 4.5 shows that the modifier / extender M3 had very little to no impact on the ductility of the base binders except in one case at 7.5% concentration. This group of binders were not evaluated after PAV aging due to the limitations in the scope of this work.

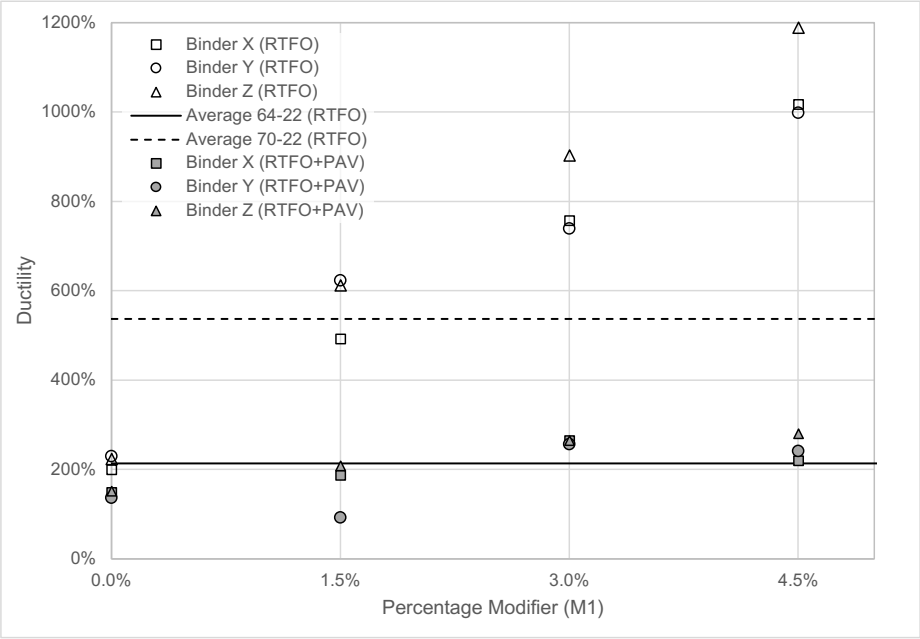

Figure 4.3. Influence of elastomeric polymer modifier on the ductility of three different asphalt binders at three different concentration levels.

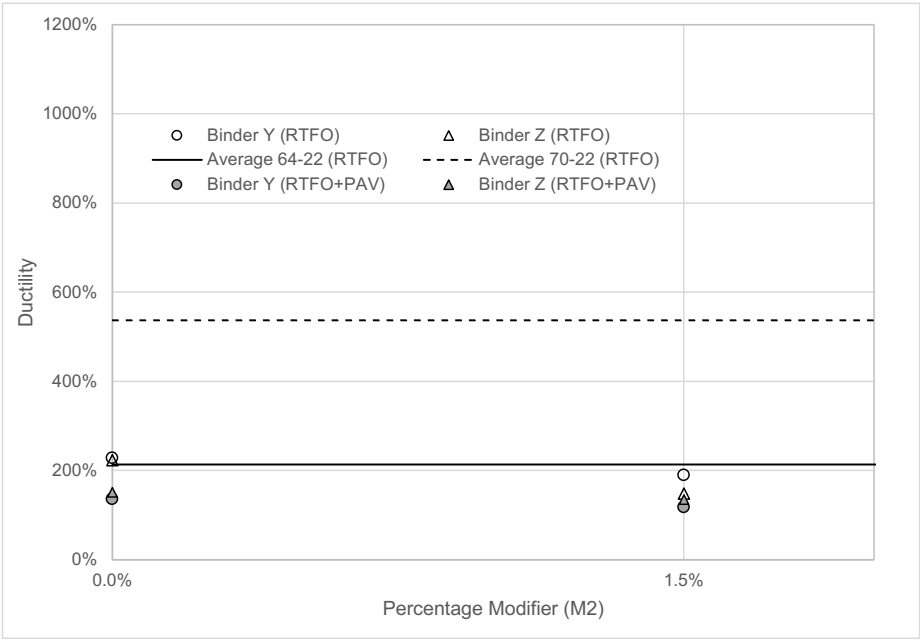

Figure 4.4. Influence of chemical modifier on the ductility of two different asphalt binders at 1.5% by weight concentration.

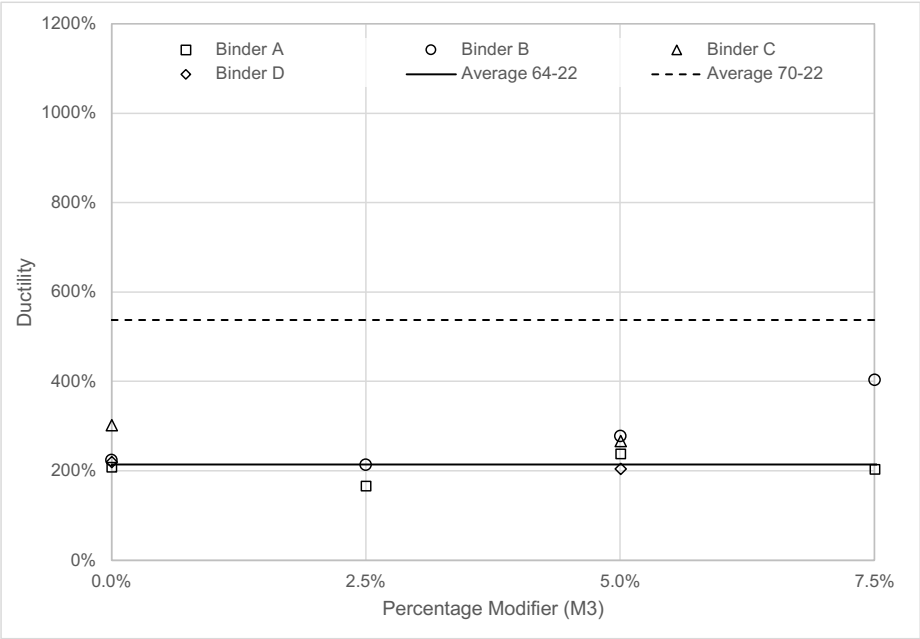

Figure 4.5. Influence of a binder modifier / extender on the ductility of four different asphalt binders; two were modified using three different percentages (2.5, 5.0, 7.5%) and the other two with one percentage (5%).

4.4 TENSILE STRENGTH VERSUS DUCTILITY

The aforementioned sections discussed the impact of PG and modifiers on the ductility of the binders as defined in the context of the poker chip test. However, as mentioned earlier, another important parameter that is obtained from this test is the tensile strength of the binder. The differences in tensile strength of the binders were not discussed explicitly in the aforementioned sections for brevity but are presented here.

Figures 4.6 and 4.7 compare the tensile strength versus ductility for Group 1 binders and Groups and 3 and 5, respectively. Figure 4.6 shows that for RTFO aged binders the ductility increases as one moves from binders with Useful Temperature Interval (UTI) of 86 to binders with UTI 92 and higher. However, more interestingly, the tensile strength of the binders does not change substantially when only RTFO aged binders are considered. This is very likely because the use of elastomeric polymers enhance ductility but do not necessarily impact tensile strength. The above statement is verified when one examines Figure 4.7 for the M1 modified binders that are only RTFO aged. For most RTFO aged binders the increase is observed in ductility and not in tensile

strength. Interestingly, on this same figure, one can also see that for the M2 modified binders, the ductility did not change or slightly decreased but resulted in an increase in the tensile strength of the binder.

A second key observation from these results is that the tensile strength of the binders increases and ductility decreases with aging. This is consistent across all binders even though the rate of change and starting point, especially the staring point for modified or PG70, 76 binders, can be very different.

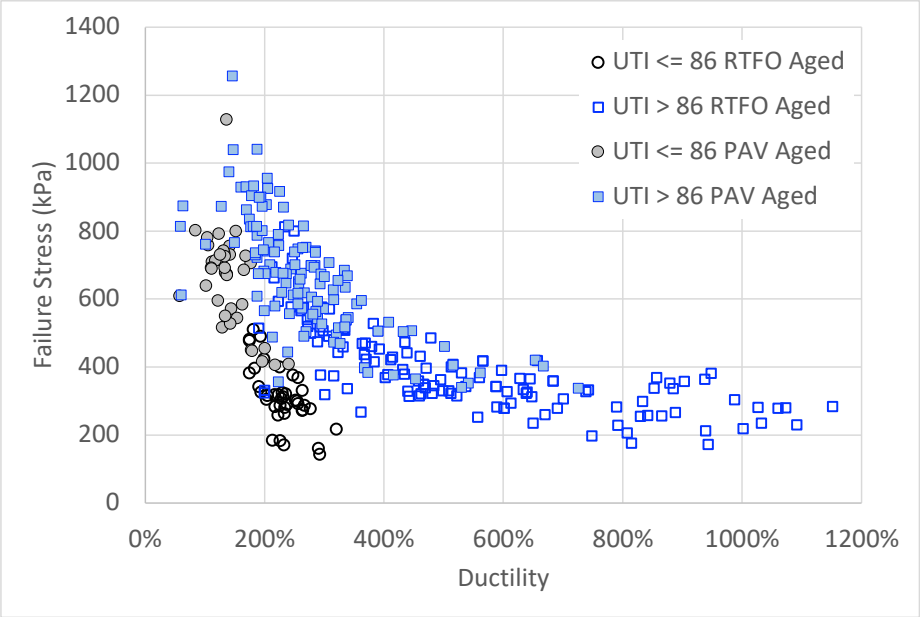

Figure 4.6. Comparison of tensile strength and ductility of PG binders.

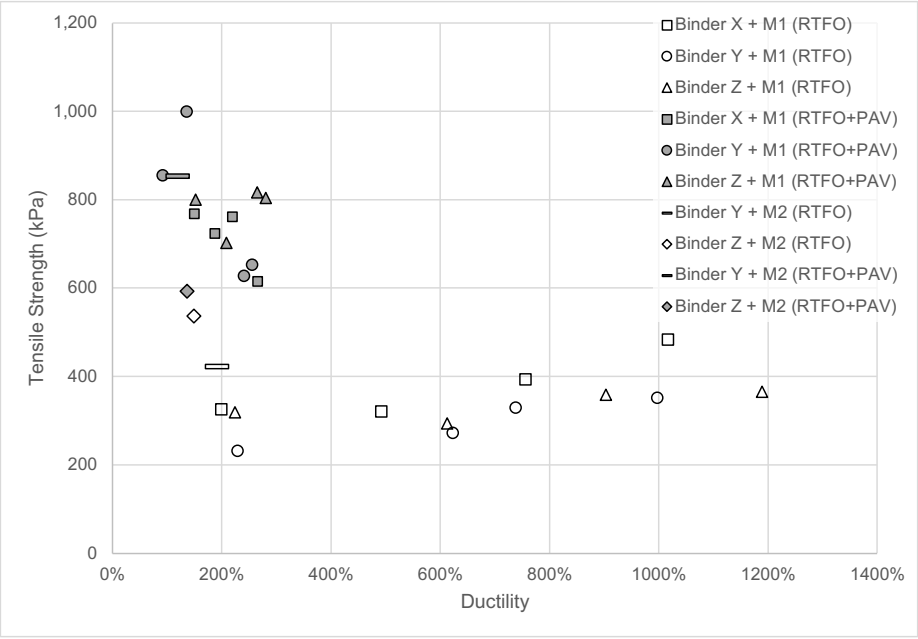

Figure 4.7. Comparison of tensile strength and ductility of binders modified using M1 (elastomer in varying percentages including control) and M2 (chemical).

CHAPTER 5. RESULTS FROM FIELD CORES

5.1 OVERVIEW

This chapter presents the results from evaluating all the binders extracted from field cores.

Cracking information presented was extracted from the most recent database developed for TxDOT Project 0-6658 Flexible Pavements and Overlays (Walubita et al., 2017). The database references both TxDOT's Pavement Management Information System (PMIS) Rater's Manual as well as the Distress Identification Manual for the Long-Term Pavement Preservation Program (LTPP) as the basis to estimate pavement distress (Texas Department of Transportation, 2016). The three main distresses of interest in this study were: (1) alligator cracking due to fatigue, (2) transverse cracking, and (3) reflective cracking of the surface layer due to pre-existing cracks from the underlying surface. These distresses were quantified according to TxDOT's PMIS Rater's Manual as briefly summarized below.

Alligator cracking is measured along each wheel path and reported as percentage of total length of test section. Though the transverse cracking recorded in accordance with PMIS Rater's Manual should include reflective cracking caused by joints and cracks under the surface, reflective cracking was reported separately by Walubita et al. (2017). It should be noted that all sections considered in this study consisted of flexible layers under the surface and therefore reflective cracking presented in the results are due to cracks in the underlying layers. The number of all transverse cracks are recorded as a count along with the average crack length and crack spacing through the test section. Reflective cracking is reported as count and percentage. The PMIS Rater's Manual requires the assessed number of transverse cracks to use a lookup table to determine the number of cracks per station (100 feet).

5.2 RESULTS

An important factor to emphasize before presenting and interpreting the test results is that the comparisons of different forms of cracking to asphalt binder ductility are being made regardless of: (i) the geographic region of the sections (warm-dry, warm-

wet, cold-dry, cold-wet), (ii) low temperature that varied from 2°F to 47°F, (iii) binder content that varied from 4.8% to 8.5%, (iv) recycled binder content that varied from 0% to 24%, (v) layer thickness that varied from 1" to 3", (vi) total HMA thickness that varied from 2" to 13.5", and (vii) cumulative ESALs during the monitoring period that varied from 0.12 million to 5 million). Figures 5.1 through 5.4 compare the ductility measured using the poker chip test to the distresses observed using the 2019 update of a field performance database corresponding to Walubita et al. (2017).

All of the six sections that showed fatigue or alligator cracking (Figure 5.1), had a ductility value below 150%. Note that this was regardless of other confounding factors such as traffic volume (illustrated by means of the circle size on the figure) and binder content (illustrated bu the circle color on the figure). Conversely, 43% of the sections that had a ductility below 150% showed some degree of alligator cracking. Note that in one case, the section was reported to have no alligator cracks at approximately the same time as the cores were obtained but had resulted in a binder ductility of 130%. Subsequent images acquired from Google© street view approximately two years later showed significant amount of cracking had emerged along the wheel path that had been sealed (Figure 5.8).

Figure 5.2 compares the poker chip ductility to the fatigue cracking that was reflected from the underlying asphalt surface to the overlay. In this case 80% of the ten sections that showed such reflective cracking had ductility that was below 150%. Conversely, 57% of the sections that had a ductility below 150% showed reflective fatigue cracking from the underlying asphalt layer. Further, several sections also showed a general trend with an increase in number of reflective cracks per 100 feet that corresponded with a decrease in ductility. Note that this trend is not withstanding the fact that the test sections represent several different traffic, structural, and mixture conditions.

Figures 5.3 and 5.4 compare the number and spacing of transverse cracks to the ductility measured using the poker chip test. As before, 80% of the sections that showed transverse cracking had ductility below 150% regardless of the other factors. Conversely, 86% of the sections that had a ductility below 150% showed some degree of transverse cracking. A general trend between ductility and the number (Figure 5.3) and the spacing (Figure 5.4) of transverse cracks can also be seen in these results.

The quantitative comparisons for the ductility versus different types of cracking

Table 5.1. Indices from testing the extracted binders on an as-is basis

Section Number	Construction Year	Specified PG	ΔT_c	G-R Parameter (kPa)	High Temperature $G^* \sin\delta$ (2.2kPa) (°C)	Poker Chip Average Stress (kPa)	Poker Chip Ductility (%)
1	2011	64-22	-3.43	164.6	83.4	936	106%
2	2011	76-22	-0.96	1422	123.6	1623	42%
3	2012	76-22	-11.72	N/A	107.7	1373	51%
4	2012	70-22	-7.55	723.2	96.1	1296	93%
5	2014	64-22	-1.6	85.6	85.4	581	179%
6	2012	64-22	-4.84	413.9	87.7	1455	140%
7	2012	64-22	-13.18	138.6	86	706	212%
8	2012	64-22	-6.1	573.7	87.6	1270	107%
9	2010	76-22	-4.04	88.3	86.6	672	153%
10	2012	64-22	-2.34	86.3	81.6	597	177%
11	2010	64-22	-9.98	N/A	101	815	30%
12	2010	64-22	-10.06	N/A	111.6	733	24%
13	2014	76-22	-7.98	174.6	84	636	177%
14	2010	64-22	-2.32	167.9	83.3	887	179%
15	2014	64-22	-9.55	627.7	94.3	N/A	143%
16	2010	64-22	-9	73.3	82.9	543	284%
17	2012	64-22	-6.29	435.7	89.6	1113	130%
18	2011	58-22	-3.83	38.8	78.4	541	214%
19	2011	70-28	-9.45	2724.9	113.5	1409	22%
20	2012	70-28	-18.81	22.1	82	N/A	50%
21	2012	70-22	-0.05	450.5	90.5	1358	53%
22	2012	N/A	-5.61	868.4	91.9	1662	75%

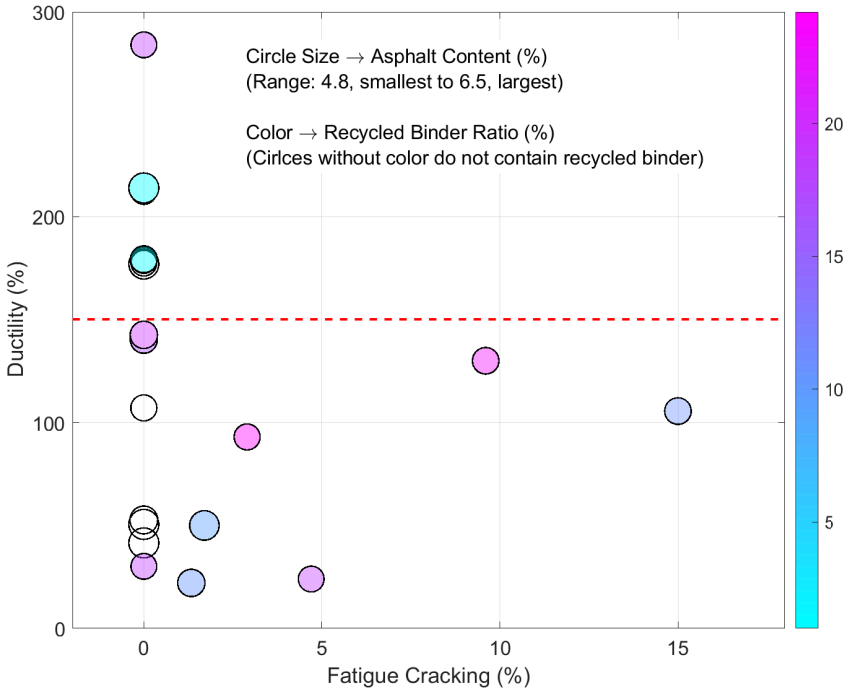

Figure 5.1. Ductility from the poker chip test versus fatigue cracking observed on the pavement; cracking measurements are from 2019 update of the data set corresponding to Walubita et al. (2017)

clearly demonstrate the importance of loss of ductility measured using the poker chip test on the likelihood of cracking of the asphalt pavement section regardless of the other traffic, environment, and mixture related factors. To further supplement these comparisons, Figures 5.5 through 5.10 illustrate a typical section of the pavement along with the corresponding ductility values (two examples each with high, medium, and low ductility values with pavements that have been in service for seven or more years) in decreasing order of ductility. A full catalog of the section images and corresponding ductility values can be found in Appendix B of this report.

In addition to the ductility measured using the poker chip test, there are parameters from other recent studies that have also been regarded as an indicator for cracking resistance of asphalt binders. Notably, as described in an earlier chapter, two parameters that were also evaluated in this study were the ΔT_c parameter and the G-R parameter. Figures 5.11 through 5.14 compare the results from the two aforementioned

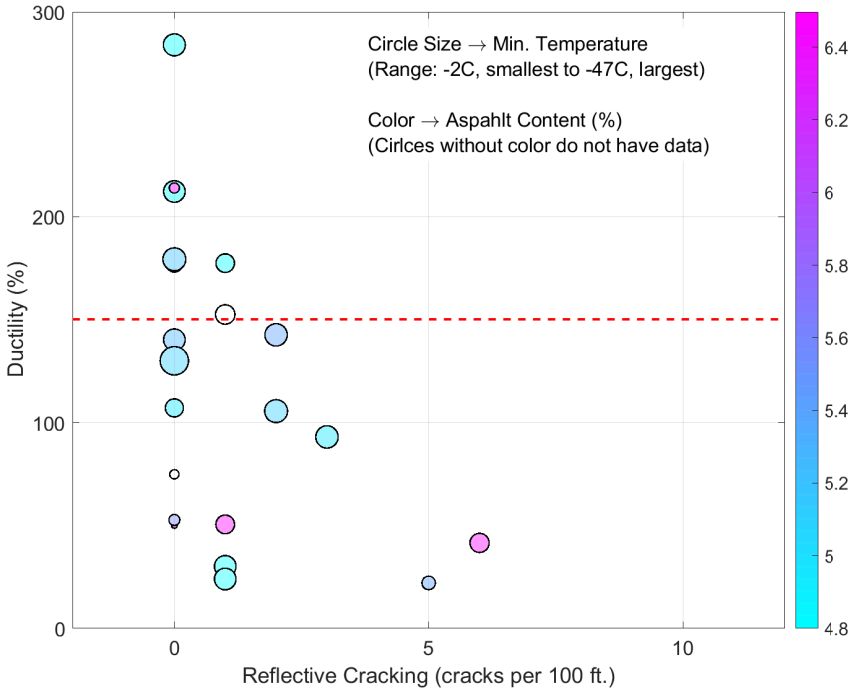

Figure 5.2. Ductility from the poker chip test versus reflective cracking observed on the pavement; cracking measurements from 2019 update of the data set corresponding to Walubita et al. (2017)

parameters with the observed distress in the field. Note that the G-R parameter could not be determined for three of the sections where the extracted binder was very stiff and resulted in master curves with unacceptable noise.

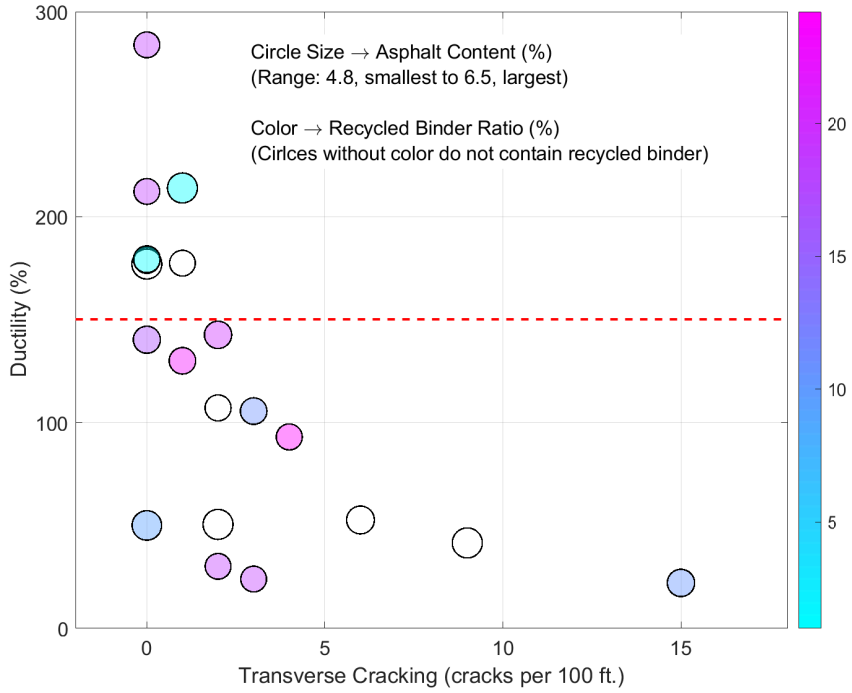

Figure 5.3. Ductility from the poker chip test versus number of transverse cracks observed on the pavement; cracking measurements from 2019 update of the data set corresponding to Walubita et al. (2017)

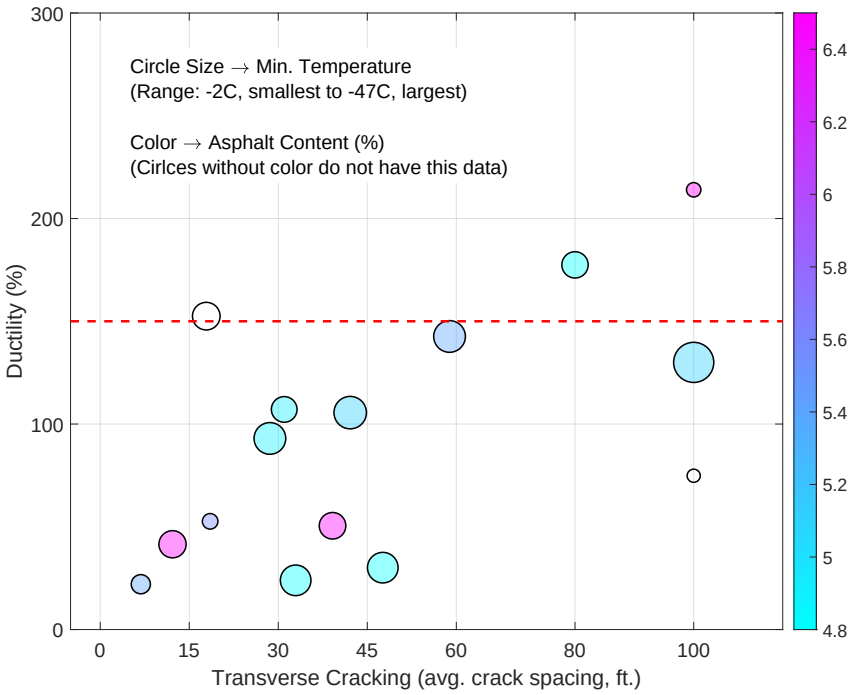

Figure 5.4. Ductility from the poker chip test versus spacing of transverse cracks observed on the pavement; cracking measurements from 2019 update of the data set corresponding to Walubita et al. (2017)

Figure 5.5. Section #18, 7 years at the time of coring, photo and coring from October 2019, no cracking was observed at the time of coring

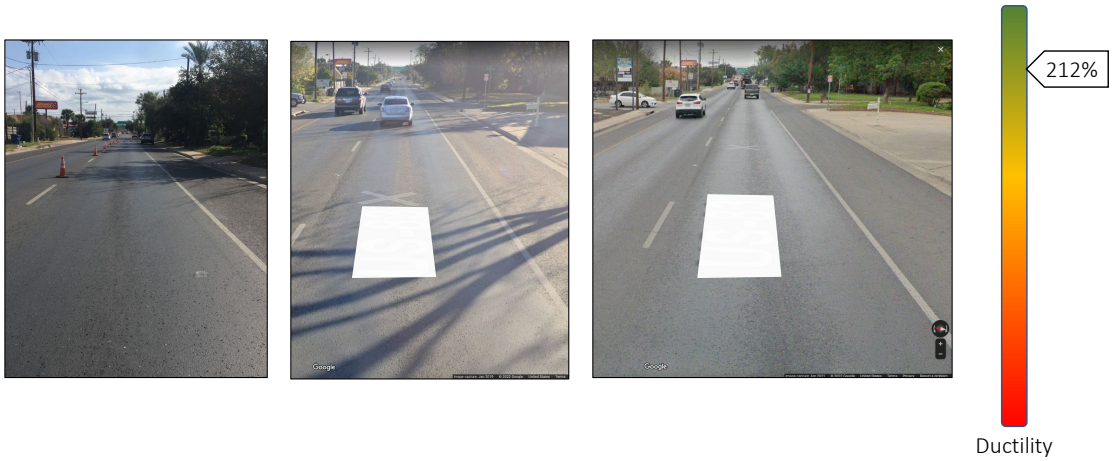

Figure 5.6. Section #7, 7 years at the time of coring, left - photo and coring from November 2021, middle and right - Google street views from January 2019 and April 2021 prior to coring showing no cracking over time

Figure 5.7. Section #6, 7 years at the time of coring, left - photo and coring from November 2021 after a recent overlay, Middle and Right - Google street view from April 2021 before the overlay was placed showing cracking along the wheel path

Figure 5.8. Section #17, 6 years at the time of coring, left - photo and coring from November 2019 when there were no apparent surface cracks, Middle and Right - Google street view from December 2021 showing cracks along the wheel path that have already been sealed

Figure 5.9. Section #12, 9 years at the time of coring, photo and coring from November 2019

Figure 5.10. Section #19, 7 years at the time of coring, left - phot and coring from March 2020 after a recent seal coat showing some bleed through cracks, middle and right - Google street view from April 2018 before the seal coat was placed showing extensive cracking

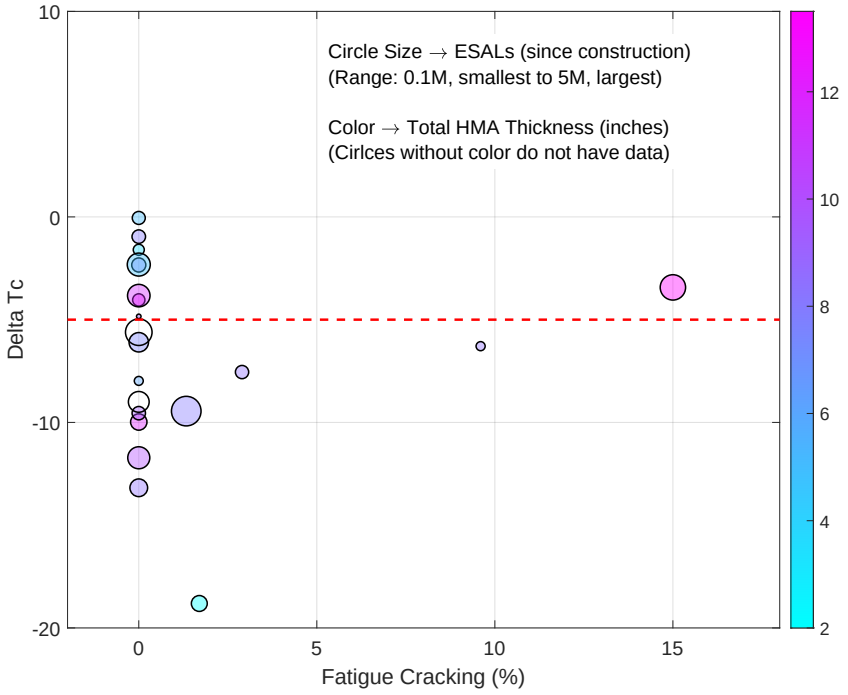

Figure 5.11. ΔT_c **versus fatigue cracking observed on the pavement; cracking measurements from 2019 update of the data set corresponding to Walubita et al. (2017)**

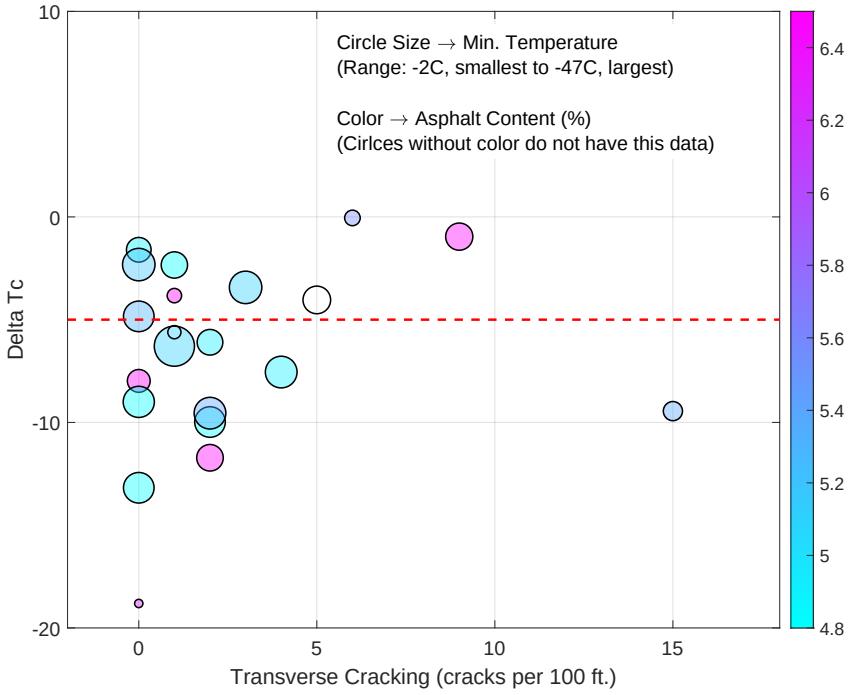

Figure 5.12. ΔT_c **versus transverse cracking observed on the pavement; cracking measurements from 2019 update of the data set corresponding to Walubita et al. (2017)**

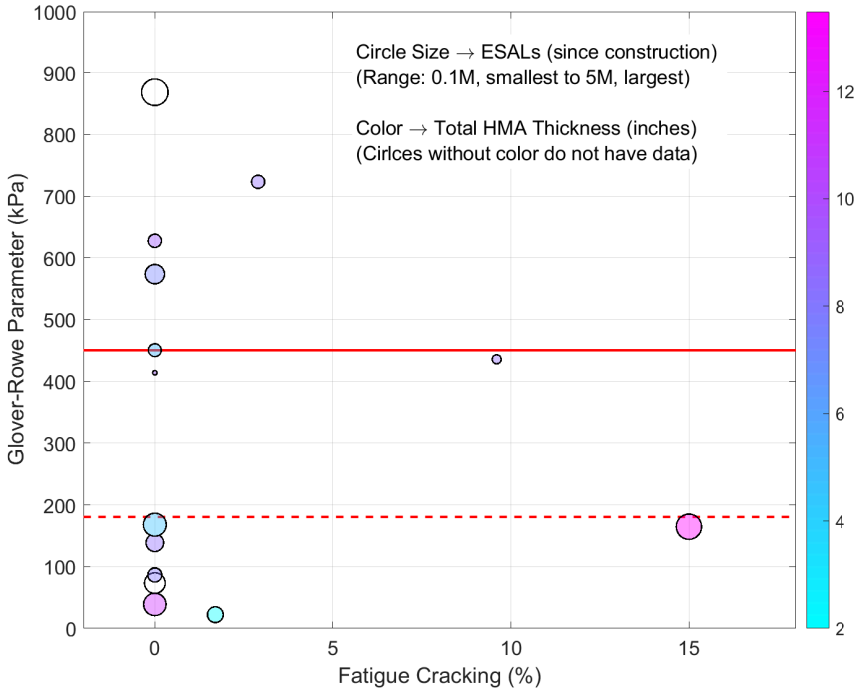

Figure 5.13. G-R parameter versus fatigue cracking observed on the pavement; cracking measurements from 2019 update of the data set corresponding to Walubita et al. (2017)

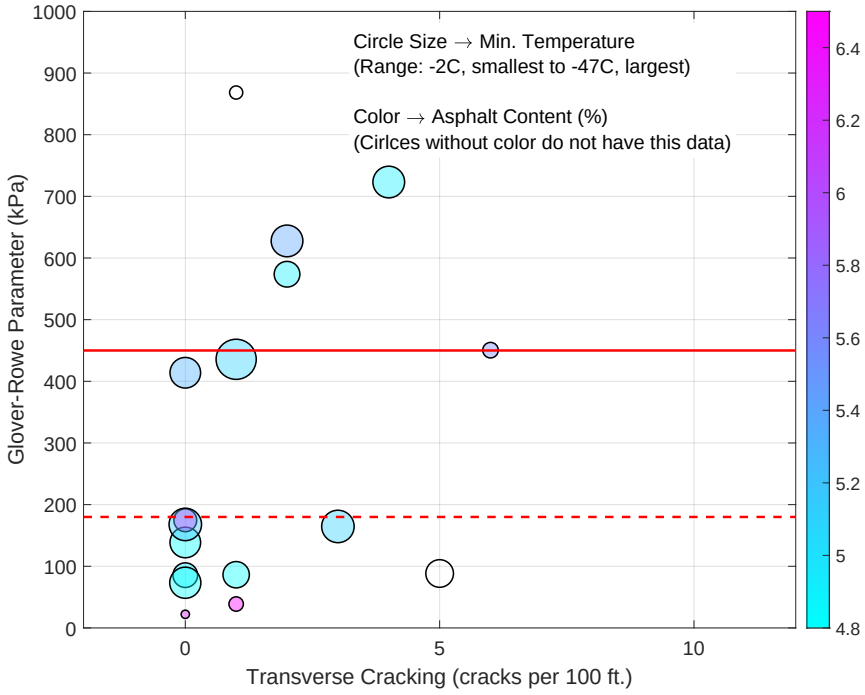

Figure 5.14. G-R parameter versus transverse cracking observed on the pavement; cracking measurements from 2019 update of the data set corresponding to Walubita et al. (2017)

CHAPTER 6. CONCLUSIONS

6.1 OVERVIEW

This study presents a simple method to measure the ductility of an asphalt binder. From a technical stand point, the proposed method (i) creates high triaxiality in the test specimen, which is a more realistic representation of the state of stress in an asphalt binder when it experiences fatigue or fracture in an asphalt mixture and (ii) evaluates the binder until complete failure. From a practical stand point, the proposed method is sensitive to a variety of different factors (e.g. aging, modifier), repeatable, and can be easily performed and analyzed. Other variations of this test method (e.g. different modes of loading) can be used for more fundamental evaluation of binders and modifiers.

6.2 SUMMARY OF FINDINGS

The proposed method and parameter were used to evaluate several different commercial and laboratory blended asphalt binders to examine the sensitivity of the method and parameter. Based on the results presented in this study, the test method and ductility parameter are both sensitive to variations in binder composition and modification. The proposed method and concomitant ductility parameter:

- can distinguish differences within binders of the same PG,
- can distinguish between the quality of RAP binders from different stockpiles,
- is very sensitive to the type and concentration of modifier, and
- can be used to assess the impact of blending RAP, modifiers, and other additives on the mechanical response of the binder.

The proposed method was also validated using the 22 field sections from across the state. The key findings from these studies are:

- All of the six sections that showed fatigue or alligator cracking had a ductility value below 150%. Conversely, 43% of the sections that had a ductility below 150% showed some degree of alligator cracking. In one case, the section was reported to have no alligator cracks at approximately the same time as the cores were obtained but had resulted in a binder ductility of 130%. This section

showed significant cracking when examined approximately two years later.

- Nearly 80% of the ten sections that showed reflective cracking from underlying HMA had ductility that was below 150%. Conversely, 57% of the sections that had a ductility below 150% showed reflective fatigue cracking from the underlying asphalt layer. A general trend between loss in ductility an an increase in reflective cracking is also seen.
- Nearly 80% of the sections that showed transverse cracking had ductility below 150% regardless of the other factors. Conversely, 86% of the sections that had a ductility below 150% showed some degree of transverse cracking. A general trend between loss in ductility an an increase in transverse cracking is also seen.
- Overall, 86% of sections with ductility below 150% showed some form of cracking. These results strongly demonstrate the ability of the poker chip test to serve as an indicator for cracking susceptibility of asphalt. These comparisons were made regardless of: (i) the geographic region of the sections (warm-dry, warm-wet, cold-dry, cold-wet), (ii) low temperature that varied from 2°F to 47°F, (iii) binder content that varied from 4.8% to 8.5%, (iv) recycled binder content that varied from 0% to 24%, (v) layer thickness that varied from 1" to 3", (vi) total HMA thickness that varied from 2" to 13.5", and (vii) cumulative ESALs during the monitoring period that varied from 0.12 million to 5 million).

6.3 LIMITATIONS AND FUTURE WORK

The results reported in this study were from tests conducted by three different researchers. For a limited number of cases, multiple replicates of the same binder were evaluated by all three researchers and no systematic differences in variability were observed. However, all tests were conducted using the same loading frame (servo-hydraulic actuator with a 25 kN load frame). In addition, approximately 10 binders were evaluated using this load frame as well as another low-cost load frame (electric motor actuator with a 5 kN load frame). The results were consistent across both units, although additional data are being gathered for a more thorough evaluation to accommodate the relatively slower motor speeds. Results from both machines and multiple operators suggest a low barrier to implementation in the future for routine use. Additional data to establish intra- and inter-lab variability will be required and performed in the future.

This study presented data from the poker chip test and the ability of this test to measure tensile strength and ductility with excellent sensitivity to material types. Although previous literature suggests correlation of ductility with field cracking, additional and more direct field validation of the parameters is required and is being carried out as a part of an ongoing study.

REFERENCES

Bennert, T., Ericson, C., Pezeshki, D., Shamborovskyy, R., and Bognacki, C. (2017). Moving toward asphalt binder and mixture protocols to minimize fatigue cracking on asphalt airfields. *Transportation Research Record*, 2633:117–126.

Christensen, D. W. and Tran, N. (2022). Relationships between the fatigue properties of asphalt binders and the fatigue performance of asphalt mixtures.

Clark, R. (1958). Practical results of asphalt hardening on pavement life. *Journal of the Association of Asphalt Paving Technologists*, 27:196–208.

Doyle, P. (1958). Cracking characteristics of asphalt cement. *Proc of Assoc of Asphalt Paving Technologists*, 27:581–597.

Glover, C. J., Davison, R. R., Domke, C. H., Ruan, Y., Juristyarini, P., Knorr, D. B., and Jung, S. H. (2005). Development of a new method for assessing asphalt binder durability with field validation.

Hajj, R. and Bhasin, A. (2018). The search for a measure of fatigue cracking in asphalt binders - A review of different approaches. *International Journal of Pavement Engineering*, 19(3):205–219.

Halstead, W. J. (1962). The relation of asphalt ductility to pavement performance. *Association of Asphalt Paving Technologists*, 32:247.

Hazlett, D. (2020). Personal communication.

Heukelom, W. (1966). Observations on the rheology and fracture of bitumens and asphalt mixes. *Association of Asphalt Paving Technologists*, 35:358.

Kandhal, P. S. (1977). Low temperature ductility in relation to pavement performance. pages 95–106. Philadelphia, PA.

Kandhal, P. S. and Koehler, W. (1987). Effect of rheological properties of asphalts on pavement cracking. *ASTM STP*, 941.

Mohammed, I., Charalambides, M., and Kinloch, A. (2016). Modeling the effect of rate and geometry on peeling and tack of pressure-sensitive adhesives. *Journal of Non-Newtonian Fluid Mechanics*, 233:85–94.

Rowe, G. M., King, G., and Anderson, M. (2014). The Influence of Binder Rheology on the Cracking of Asphalt Mixes in Airport and Highway Projects. *Journal of Testing and Evaluation*, 42(5).

Sultana, S., Bhasin, A., and Liechti, K. M. (2014). Rate and confinement effects on the tensile strength of asphalt binder. *Construction and Building Materials*, 53:604–611.

Texas Department of Transportation (2016). Pavement management information system, rater's manual.

Walubita, L. F., Lee, S. I., Faruk, A. N., Scullion, T., Nazarian, S., Abdallah, I., et al. (2017). Texas flexible pavements and overlays: year 5 report-complete data documentation. Technical report, Texas A&M Transportation Institute.

Zhang, R., Zhang, W., Shen, S., Wu, S., and Zhang, Y. (2021). Evaluation of the correlations between laboratory measured material properties with field cracking performance for asphalt pavement. *Construction and Building Materials*, 301.

APPENDIX A. STEP-BY-STEP PROCEDURE TO PREPARE A POKER CHIP TEST SPECIMEN

The following steps are to be followed to prepare a poker chip test specimen.

1. Heat container with the asphalt binder sample to be tested (typically a 2 oz. metal can) to 160°C for 15 to 20 minutes or until the binder is fluid enough to be poured. For short-term aged binders, a sample can also be obtained immediately after completing the RTFO procedure by directly pouring from the hot RTFO bottle. It is important to note that for high polymer modified binders and/or samples being tested after PAV aging, a slightly higher temperature may be necessary to ensure that the sample is completely fluid and well mixed.
2. Stir the sample in the can or container to ensure it is homogeneous. **IMPORTANT:** this is a very important step because polymer modified samples can separate after heating (particularly if the sample container has been in storage for long).
3. The step allows the person testing to pre-weigh multiple samples for testing in a batch subsequently (Figure A.1). Pour 4.5 ± 0.05 g of the asphalt binder in a silicon mold and allow it to cool to room temperature. When pouring more than two or three samples from the same container at the same time, it is important to ensure that the binder in the can has not cooled down to a point where it does not flow well. In such cases, it may be better to reheat the can for a couple of minutes again. Ensure that the mold is appropriately labelled.

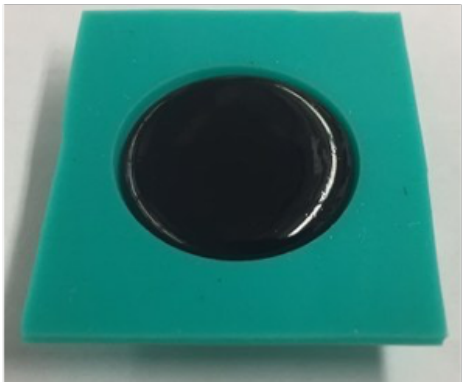

Figure A.1. Silicone mold to weight and store the sample for further testing.

4. Wipe the test surface of the poker chip plates (top and bottom) using Acetone and ensure that the surfaces are clean without any residue from previous tests or cleaning agent. **IMPORTANT:** This is an important step because any traces of contaminants on the surface remaining after cleaning or from the previous tests will interfere with the test results.
5. Preheat the top and bottom plates in an oven at 160°C for at least 45 minutes. It may be easier to place multiple poker chip plates in a flat tray and use the tray to transfer the fixtures in and out from the oven. Also place the spacer dowels in a can and place the can inside the oven along with the poker chip fixtures. **IMPORTANT:** Ensure that the oven trays are level using a bubble level prior to use.
6. Remove the pre-heated poker chip plates from the oven and transfer the pre-weighed dollop of the binder from the silicon mold to the bottom plate of the poker chip mold (Figure A.2) and place it back in the oven. This will allow the binder sample to flow and spread over the bottom plate.

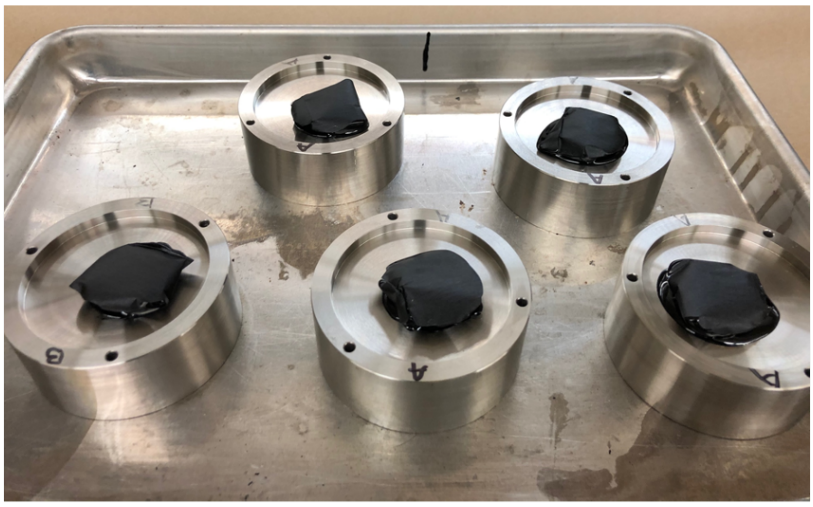

Figure A.2. Binder samples from the silicone mold placed into heated bottom plate of the poker chip assembly.

7. Place the sample back in the oven set at 160°C and wait for 15 minutes or until the dollop of binder has completely molten and spread over the entire plate.
8. Remove the molds from the oven and place three spacer pins approximately at 120 degrees apart and about half way radially out from the center.

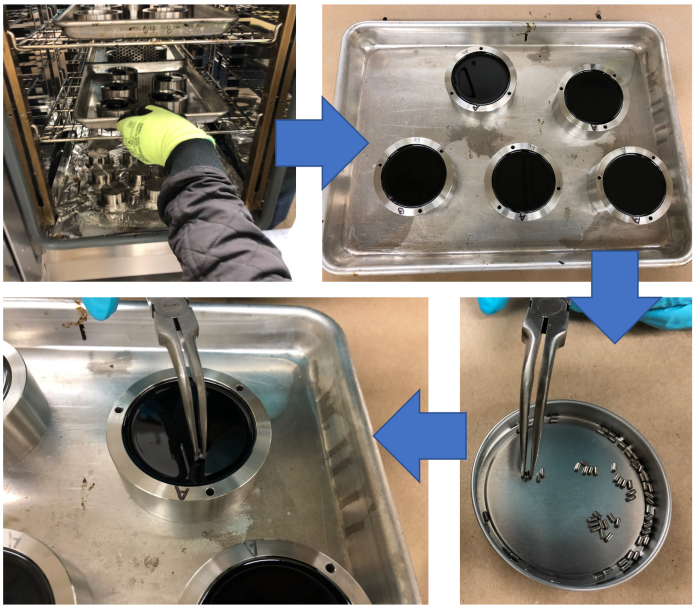

Figure A.3. Placement of dowels for film thickness control on liquid binder in the heated bottom plate of the poker chip assembly.

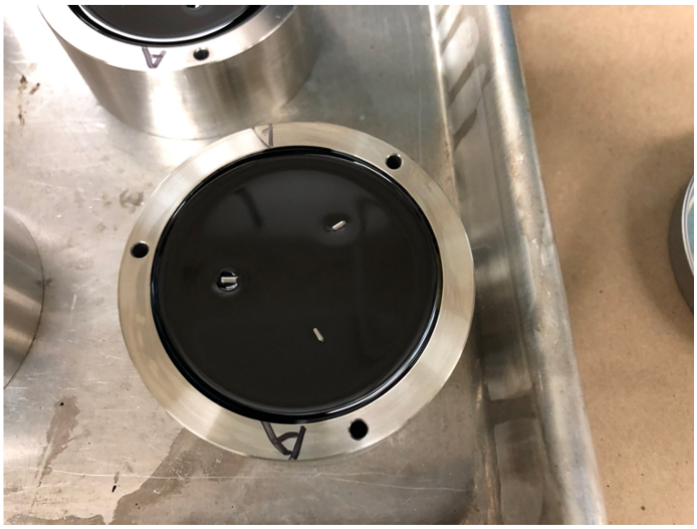

Figure A.4. Closer view of three dowels used for film thickness control placed on the liquid binder in the heated bottom plate of the poker chip assembly.

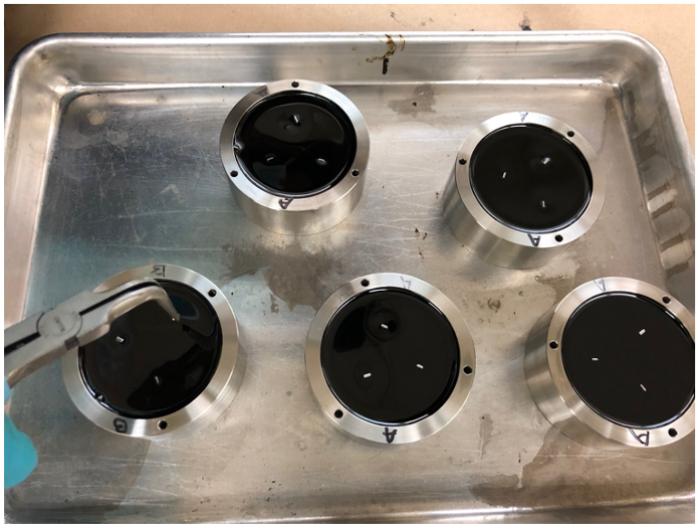

Figure A.5. Multiple samples being prepared for testing.

9. Place the bottom plate back in the oven for another 5 minutes to allow the spacer dowels to sink and submerge in the binder. The spacer dowels will only partially submerged due to surface tension of the asphalt binder.
10. Remove the bottom part and the pre-heated top part of the mold from the oven. Place two alignment pins in the lower part of the mold. Lower the top part of

the poker chip mold slowly through the alignment pins and firmly press it at the center to ensure a correct set. Place the third alignment pin to ensure proper alignment. **IMPORTANT:** Exercise caution, the plates are hot and the binder is fluid; dropping the top plate suddenly may cause the hot binder to splatter.

11. Place the assembled poker chip specimen back in the oven for 15 minutes to allow bonding between the binder and the face plate.
12. Place the poker chip fixture on a level platform to cool to the test temperature prior to testing.

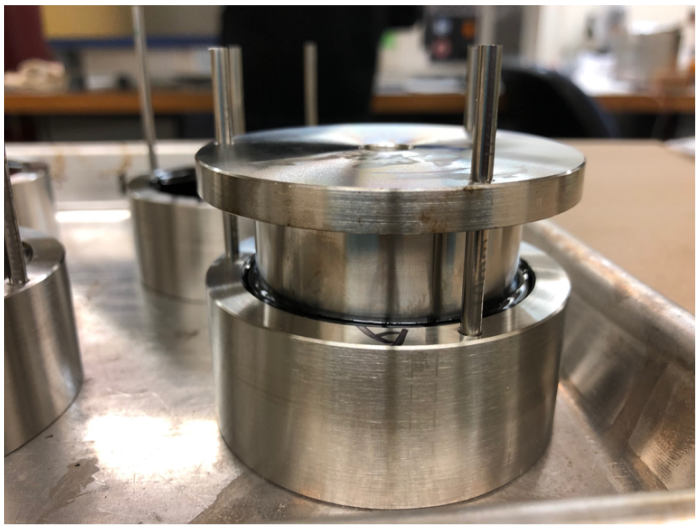

Figure A.6. Side of the poker chip assembly after placing the top plate and alignment pins.

APPENDIX B. IMAGES FROM DIFFERENT FIELD SECTIONS WITH DUCTILITY VALUES IN ORDER OF DECREASING DUCTILITY

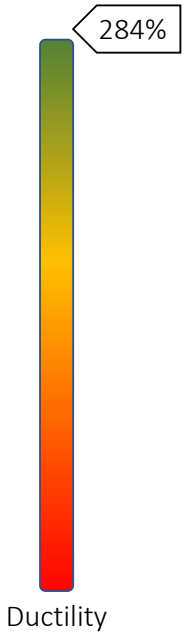

Section #16: 4 years
Photo and coring from Nov. 2021

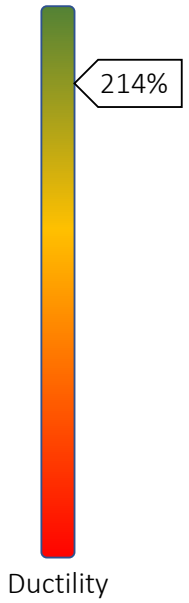

Section #18: 7 years
Photo and coring from Oct. 2019

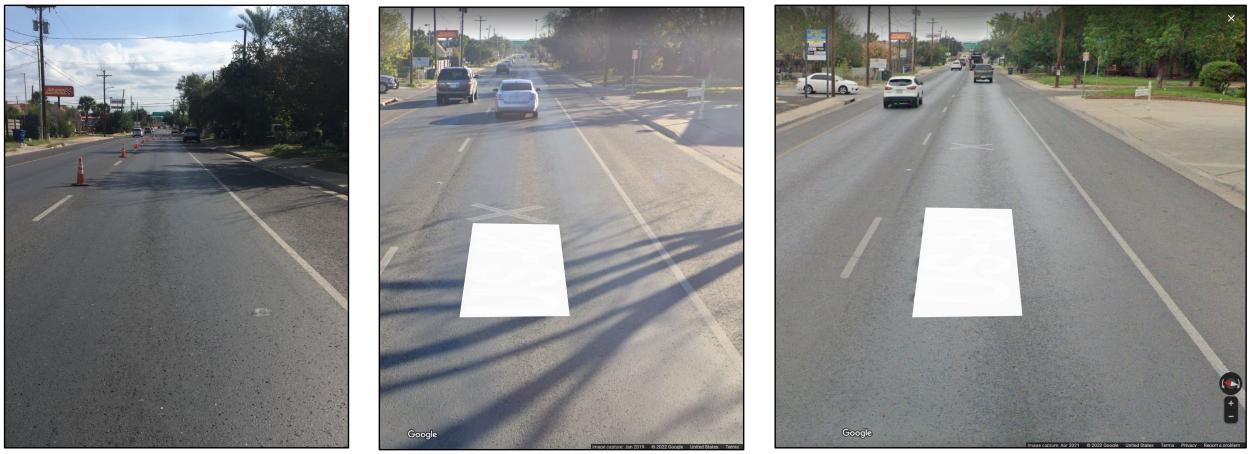

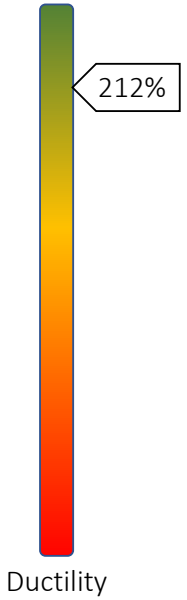

Section #7: 7 years
Left – Photo and coring from Nov. 2021; Middle and Right – Google Street from Jan. 2019 and April 2021 showing no cracking over time

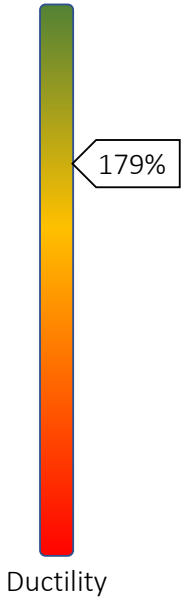

Section #5: 5 years
Photo and coring from Dec. 2019 after seal coat was placed

Section #14: 8 years
Left – Photo and coring from Dec. 2019; Right – Google Street, Apr. 2021

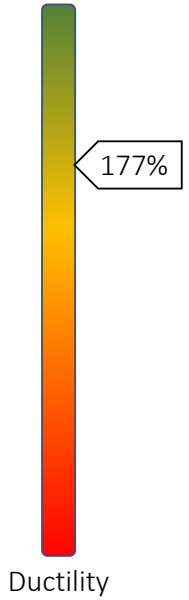

Section #10: 7 years
Photo and coring from Dec. 2019

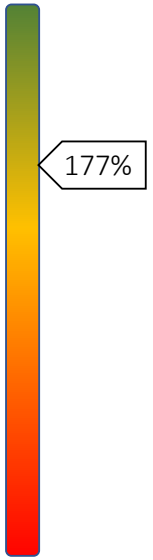

Section #13: 4 years
Photo and coring from Dec. 2019

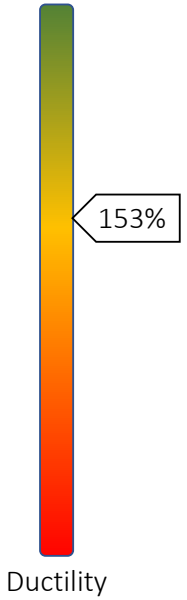

Section #9: 9 years
Photo and coring from Dec. 2019 as cracks are beginning to emerge

Section #15: 4 years
Photo and coring from Nov. 2019 as cracks are beginning to emerge

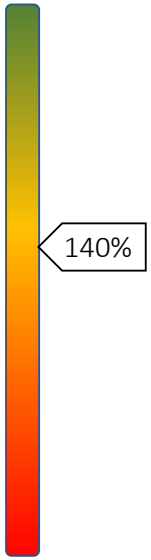

Section #6: 7 years
Left – Photo and coring from Nov. 2021 after a recent overlay; Right – Google Street from April 2021 before the overlay showing cracking

Section #17: 6 years
Note: Left – Nov. 2019 during coring; Middle and Right – Google Street, Dec. 2021

Section #8: 7 years
Photo and coring from Dec. 2019, a seal coat was placed prior to coring but cracks bleeding through are visible

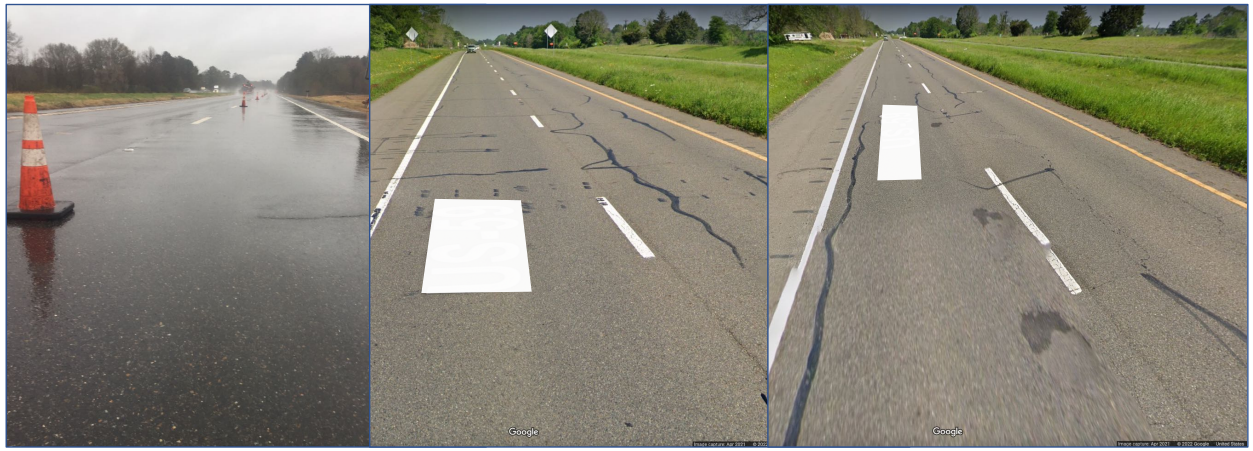

Section #1: 7 years
Left – Photo and coring from Dec. 2019; Middle and Right – Google Street, Apr. 2021

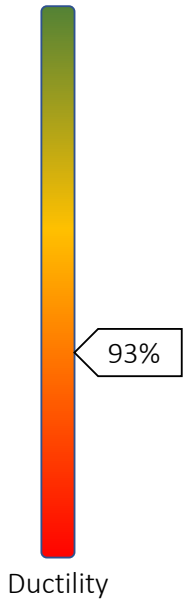

Section #4: 6 years
Photo and coring from Nov. 2019

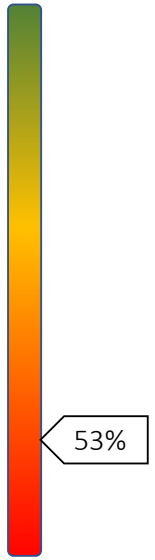

Section #21: 6 years
Left – Photo and coring from Sept. 2021 after a recent seal coat; Right – Google Street from July 2019 before seal coat showing cracks

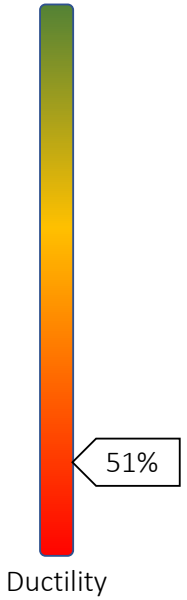

Section #3: 7 years
Photo and coring from Sept. 2021

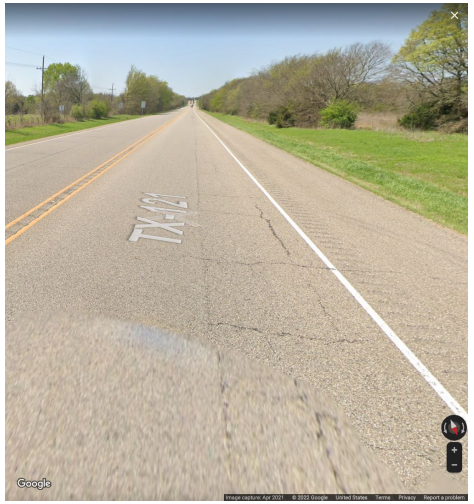

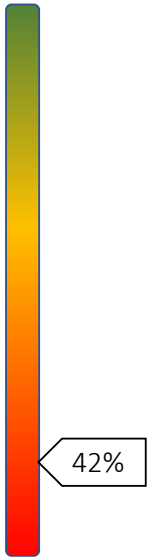

Section #2: 8 years
Left – Photo and coring from Sept. 2021; Right – Google Street from April 2021

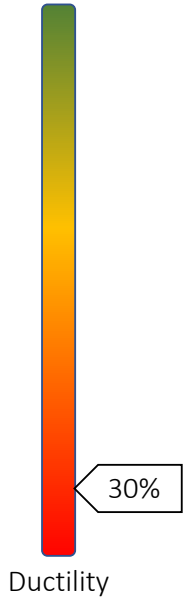

Section #11: 9 years
Photo and coring from Nov. 2021

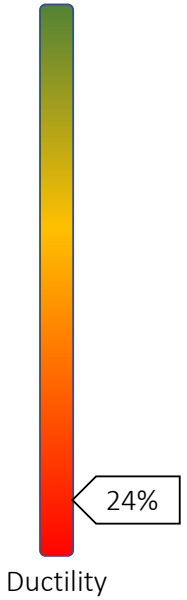

Section #12: 9 years
Photo and coring from Nov. 2021

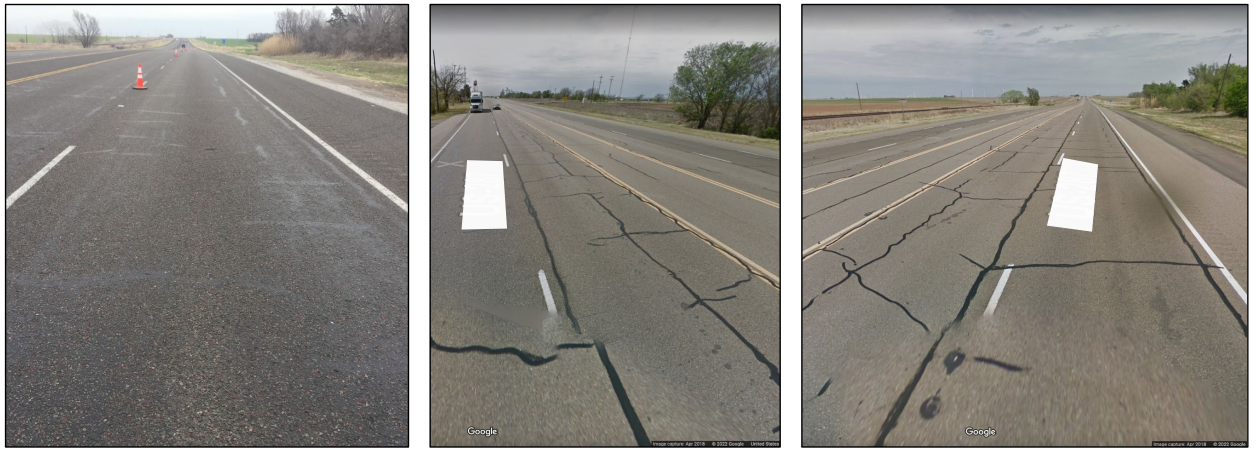

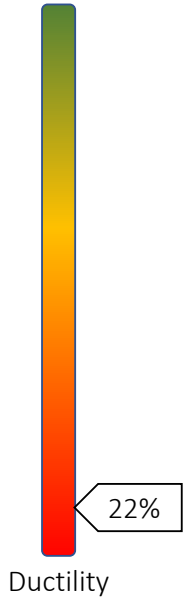

Section #19: 7 years
Left – Photo and coring from March 2020 after a recent seal coat showing some bleed through cracks; Right – Google Street from April 2018 before seal coat showing cracks

APPENDIX C. TEST METHOD FOLLOWING TXDOT AND AASHTO TEMPLATE

Test Procedure for

POKER CHIP TEST OF ASPHALT BINDER

TxDOT Designation: XXXXX

Effective Date: XXXXXX

1. SCOPE

1.1 This test method evaluates the tensile failure characteristics of an asphalt binder under a state of stress that induces high triaxiality in the asphalt binder, which models a realistic stress state similar to asphalt binder confined between two aggregates. This test method is relevant for fatigue or thermal cracking in asphalt mixtures and can be used with material aged using T 240 (RTFOT) and R 28 (PAV).

1.2 The values given in parentheses (if provided) are not standard and may not be exact mathematical conversions. Use each system of units separately. Combining values from the two systems may result in nonconformance with the standard.

2. APPARATUS

2.1 *Testing Machine* – The testing machine or load frame, as shown in Fig. 1, should have the capability of applying tension in displacement-controlled mode, and switch to load-controlled mode until the sample fails and during this time the load and displacement are recorded.

Note 1 – A servo hydraulic testing machine with a function generator capable of producing the desired displacement-controlled or load-controlled mode has been shown to be suitable for use in tension testing. Other commercially available electric motor actuator and load frame with at least 900 lbf (4 kN) load cell can also be used.

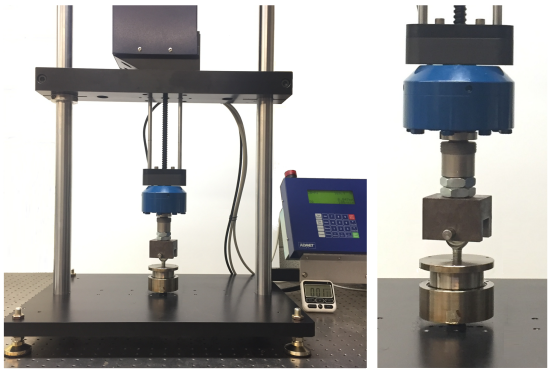

Figure 1 *- Testing Machine (left: overall view of the load frame, right: closer view of the load cell)*

Note 2 – The device should be capable of applying a displacement rate of at least 5.9 in/minute (150 mm/minute).

2.1.1 The load frame must be set up to apply tension in displacement-controlled mode of 0.04 in/minute (1 mm/minute) until a tensile load of 9 lbf (40 N) is reached. At this point the load frame must switched to a load-controlled mode to apply a tensile load of 0.25 lbf/second (2 N/second) until the sample fails. During this time the load and displacement are recorded at a rate of at least 2 points per second.

2.1.2 The testing machine must be coupled with an automatic cut off system that can be programmed using a digital controller to stop the equipment in case of emergency.

2.2 *Measurement and Recording System* – The system should include sensors for measuring and recording vertical deformations. The system should be capable of measuring vertical deformations with a resolution of at least 0.00004 in. (0.001 mm). Loads should be measured and recorded with a resolution of at least 0.0225 lbf (0.1 N).

2.2.1 The vertical deformation can be measured by a linear variable differential transducer (LVDT) or other suitable device. The sensitivity and type of measurement device should be selected to provide the deformation readout required in 2.2.

2.2.2 The load should be measured with an electronic load cell capable of satisfying the specified requirements for load measurements in 2.2.

2.2.3 Refer to the manufacturer's specifications for system calibration and accuracy.

2.3 *Temperature-Controlled Chamber for Conditioning Specimen* – The temperature-controlled chamber should be capable of maintaining a temperature of 77°F (25°C), and within 1°F (0.5°C). The chamber should be large enough to hold at least ten specimens for a period of at most 24 h prior to testing.

2.4 *Oven* – The oven must be capable of maintaining a temperature of 320 ± 5°F (160 ± 3°C).

2.5 *Stainless Steel Mold* – The poker chip sample is prepared using a two-piece mold (top and bottom) and shall be similar in design to that shown in Fig. 2 and 3. The mold shall be made of stainless steel, and dimensions of the assembled mold shall be as shown in Fig. 2 and 3, with the permissible variations indicated. Two parts of the mold, as shown in Fig. 4, are used to prepare a thin film specimen.

Note 3 – Mold thread size and depth may vary based on the mounting system of the testing machine.

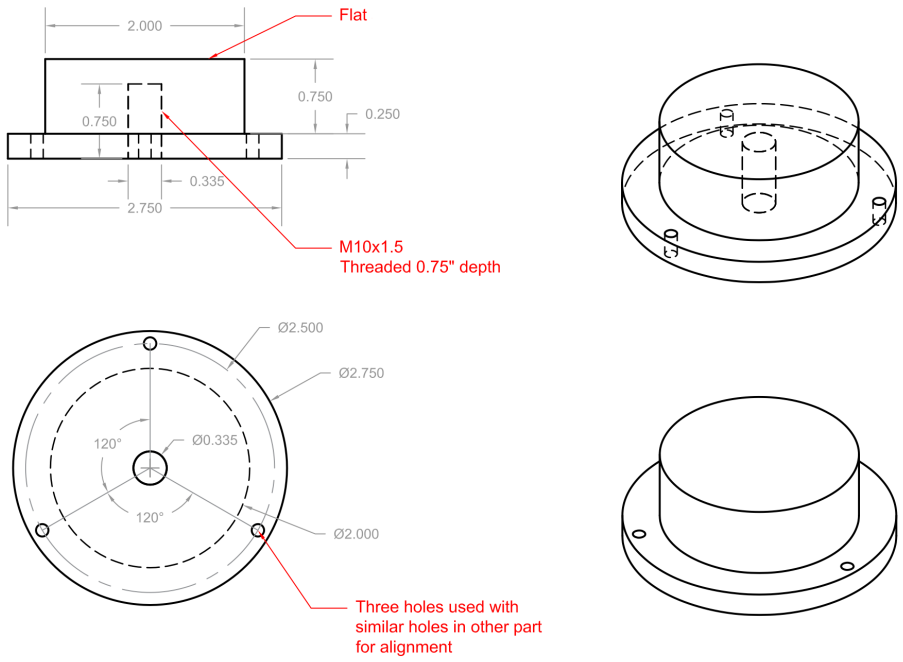

Figure 2 *– Stainless-Steel Mold. Top piece of the poker-chip mold (all dimensions in inches)*

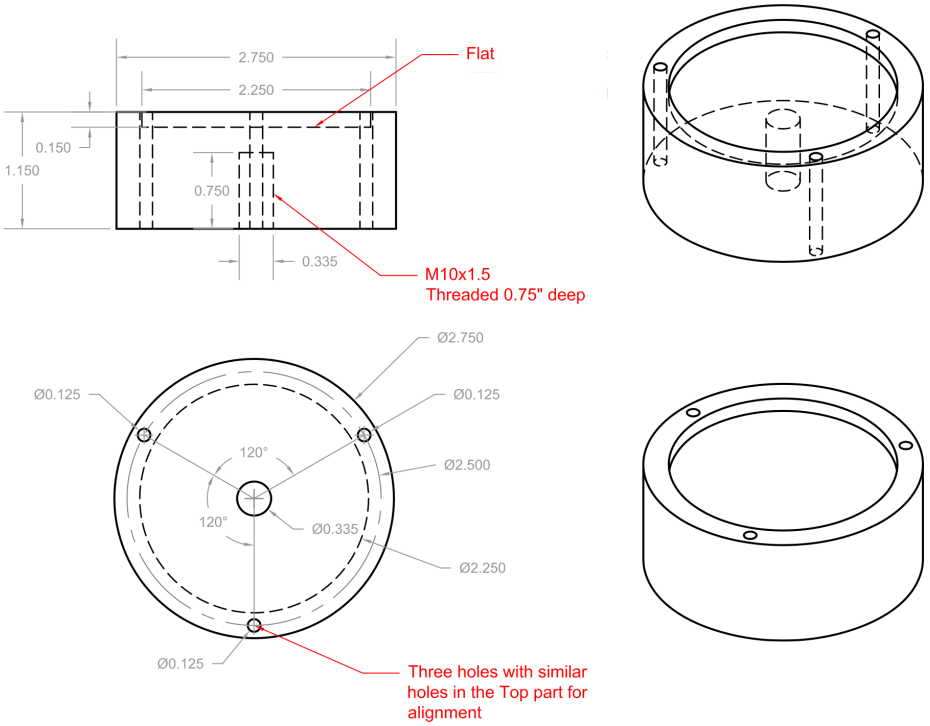

Figure 3 *– Stainless-Steel Mold. Bottom piece of the poker-chip mold (all dimensions in inches).*

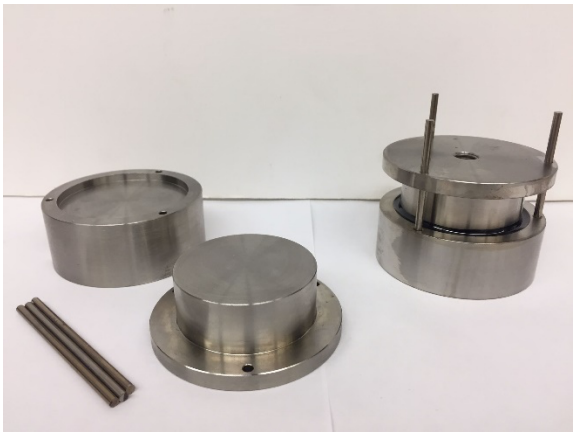

Figure 4 *– Poker chip stainless-steel mold and laboratory-molded specimen between the top and bottom pieces that are aligned using three alignment pins (top and bottom of the mold with the three alignment rods are shown to the left and an assembled mold with the binder sample is shown to the right).*

2.6 *Alignment pins* – The alignment pins can be machined or purchased directly from a hardware supplier. The pins shall be made of stainless steel and should be 0.122 ± 0.0002 in (3.1 ± 0.005 mm) diameter and 2 ¾ in (69.85 mm) length. These alignment pins are run through the three holes in the top and bottom of the poker chip specimen mold to ensure proper alignment of the two parts. Three alignment pins are needed for each poker-chip mold.

2.7 *Spacer Dowels* – The spacer dowels can be machined or purchased directly from a hardware supplier. The spacer dowels shall be made of alloy steel and should be 1/16 ± 0.0003 in (0.0025 ± 1.18E-05 mm) diameter and 1/8 in (0.005 mm) length. These spacer dowels are dropped in the liquid asphalt binder to achieve the target thickness when placing the top piece of the poker chip mold.

2.8 *Ball Joint Rod End* – The ball joint rod end can be machined or purchased directly from a hardware supplier and shall be made of alloy steel with a ball joint end type. This ball joint rod end is used on the top piece of the poker chip mold to connect to the load frame using an appropriate clevis pin and dowel.

2.9 *Silicone Molds* – The silicone molds should be made of food grade silicone, bisphenol A (BPA) free, non-stick and flexible to easily release the asphalt binder from the molds. Typically, the temperature tolerance range of this material is from -40 to 466°F (-40 to 241°C). The diameter of each cavity is 1.0 in (25.4 mm) and 1/4 in (6.35 mm) depth. These dimensions hold approximately 0.159 oz (4.5 g) of asphalt binder properly.

2.10 *90 Degree Bent Nose Pliers* – The 90 degree bent nose plier is a variation of needle nose pliers. It features non-serrated tapered jaws that are bent at a 90 degree angle, 3/8" from the tip. This allows the jaws to grip the spacer dowels.

2.11 *Stainless-Steel Trays* – The stainless-steel trays should have a size of 13 x 9.5 x 1 in (330.2 x 241.3 x 25.4 mm) with a flat rigid base to accommodate up to 10 molds and carry them in and out of the oven or temperature controlled chamber.

2.12 *Acetone* – Acetone can be used to clean and remove dust from the surface of the stain-less steel and silicone molds.

2.13 *Dry wipes* – Dry paper tissue wipes provide an easy way to wipe up liquid and dust from the surface of the stainless steel and silicone molds.

2.14 *Balance* – Balance conforming to the requirements of AASHTO M 231, Class G2.

2.15 *Stainless Steel Micro Spatula* – The stainless steel spatula that is 22.5 cm (9.0 in) length and 5 x 0.78 cm (2 x 0.31 in) flat ends and mirror-like finish.

2.16 Bubble Level – The bubble level can be used to indicate whether the surface of the stainless-steal trays containing the poker-chip molds are horizontal (level).

3. MATERIALS

3.1 *Asphalt Binder Specimen* – The asphalt binder can be aged using T 240 (RTFOT) or R 28 (PAV), or both.

3.2 *Recovered Specimen* – The recovered asphalt binder from asphalt mixture or reclaimed asphalt pavement (RAP) can be tested "as is" condition or it can be aged using R 28 (PAV).

4. SPECIMENS

4.1 *Laboratory-Molded Specimen* – Condition the asphalt binder in accordance with AASHTO T 240 or TxDOT Tex-541-C (RTFOT). If long term aged asphalt binder is to be tested, obtain test sample according to AASHTO R 28 (PAV). Two circular specimens of 2.0 in (50.8 mm) diameter with a 1/16 in (1.5875 mm) thickness are prepared using the stainless steel mold described in the section above.
Note 4 – The asphalt binder is heated inside an oven until the material is sufficiently fluid. Typically, a temperature of 320 ± 5°F (160 ± 3°C) is adequate. Modified asphalt binders may be heated to higher temperatures if material does not pour easily.

5. PROCEDURE

5.1 *Asphalt Binder Sample Preparation:*

5.1.2 Heat a 2 oz (60 ml) metal can, containing the asphalt binder sample, in an oven to 320 ± 5°F (160 ± 3°C) for 15 to 20 minutes until the binder is fluid enough to be poured. During the heating process, the sample should be covered.

5.1.3 Stir the sample thoroughly to ensure it is homogenous.

5.1.4 Pour 0.159 ± 0.0018 (4.5 ± 0.05 g) of the asphalt binder inside the silicon mold, as shown in Fig. 6, label the mold and set it aside. Allow the silicon mold to cool to room temperature after pouring.
Note 6 – The same amount of asphalt binder sample can be poured directly into a clean pre-heated bottom part of the poker chip mold. However, the balance used must be insulated to protect the weighing plate from the pre-heated bottom part of the poker chip mold.

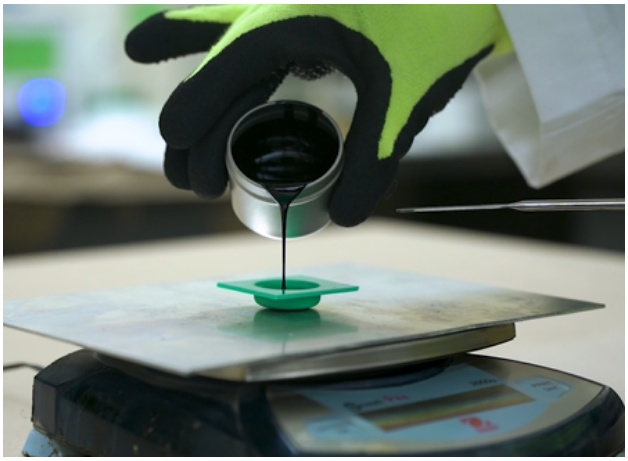

Figure 5 *- Asphalt binder poured inside the silicone mold.*

5.2 *Laboratory-Molded Specimens Preparation:*

5.2.1 Wipe and clean the top and bottom test faces of the poker chip mold using acetone.

5.2.2 Place the three alignment pins in the bottom part of the poker chip mold.

5.2.3 Preheat the top and bottom parts of the poker chip mold and the spacer dowels in a conventional oven at 320 ± 5°F (160 ± 3°C) for at least 45 minutes. The poker chip molds can also be left overnight in the oven.
Note 7 – Stainless steel trays can be used to transport the poker chip molds. Ensure that the oven trays are level using a bubble level prior to use.

5.2.4 Remove the pre-weighed dollop of the asphalt binder from the silicon mold and place it in the bottom part of the poker chip mold. Place the bottom part of the mold back in the oven at 320 ± 5°F (160 ± 3°C) for 15 minutes or until the dollop of asphalt binder has completely molten and spread over the entire bottom surface of the poker chip mold.

5.2.5 Place three spacer dowels approximately at 120 degrees apart and about halfway radially out from the center of the bottom poker-chip sample disc.
Note 8 – A 90 degree bent nose pliers can be used to grip the spacer dowels.

5.2.6 Place the bottom part of the poker chip mold back in the oven for another 5 minutes to allow the spacer dowels to sink and submerge in the binder.
Note 9 – The spacer dowels will be partially submerged due to the surface tension of asphalt binder.

5.2.7 Remove the bottom part and the pre-heated top part of the mold from the oven. Place two alignment pins in the lower part of the mold. Lower the top part of the poker chip mold slowly through the alignment pins and firmly press it at the center to ensure a correct set. Place the third alignment pin to ensure proper alignment.
Note 10 – Exercise caution. Plates are hot and the asphalt binder is fluid. Suddenly dropping the top poker-chip sample disc may cause the liquid binder to splash out.

5.2.8 Place the poker chip assembly in the oven at 320 ± 5°F (160 ± 3°C) for another 15 minutes.

5.2.9 Remove the poker chip assembly from the oven and let it cool to room temperature on a level platform.
Note 11 – If the asphalt binder spilled over, discontinue the procedure and discard the specimen.

5.2.10 Place the poker chip assembly inside the temperature-controlled chamber at 77 ± 1°F (25 ± 0.5°C). Ensure that the poker chip assembly is level using a bubble level.
Note 12 – If room temperature is within ± 1.0°F (± 0.5°C) of target temperature, the poker chip assembly can be cooled at room temperature.

5.3 *Mounting and Testing Laboratory-Molded Specimens in the Testing Machine:*

5.3.1 Ensure that the load cell of the testing machine is zeroed out with just the top part of the poker chip mold suspended from the loading axis.

5.3.2 Program the load frame to run the following sequence: i) apply tension in displacement-controlled mode of 0.04 in/minute (1 mm/minute) until a tensile load of 9 lbf (40 N) is reached, at this point ii) switch to load controlled mode and apply a tensile load of 0.25 lbf/second (2 N/second) until the sample fails.

5.3.3 Take the specimen and gently remove the alignment pins while holding the bottom of the specimen.
Note 13 – Do not use force to remove the alignment pins; if they appear stuck for any reason, gently tap using the back of a screwdriver and try to wriggle it free.

5.3.4 Check the lip of the bottom of the specimen to ensure that there is no binder that spilled over; this would indicate that the specimen was not cooled on a level platform.

5.3.5 Lock the bottom of the poker chip assembly in the loading frame.

5.3.6 Thread in the ball joint rod on the top of the poker chip mold and ensure it is finger tight but do not apply too much torque to avoid damaging the specimen.

5.3.7 Lower the loading axis gently until the clevis rod end hole aligns with the hole in the ball joint rod. Gently slide a dowel through the clevis rod end and the ball joint rod locking the two in place. Once the sample is locked in place, run the programmed test.

5.3.8 Start the test using the programmed sequence according to the section 5.3.2. The testing device automatically starts the test when the load frame has achieved a tensile load of 9 lbf (40 N).

5.3.9 Record the load and displacement at a rate of at least 2 points per second during the test. Fig. 5 shows a typical poker-chip test output data.

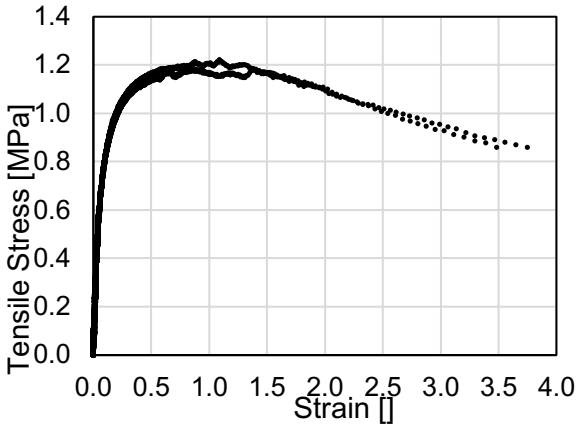

Figure 6 *– Typical Poker-chip Test Output Data*

6. CALCULATIONS

6.1 Calculate the maximum stress, S_{Tmax}, recorded as the tensile strength as follows:

$$S_{Tmax} = \frac{4\,P_{ult}}{\pi D^2}$$

where:
P_{ult} = ultimate applied load required to fail specimen, lbf (or N), and
D = diameter of specimen, in (or mm).

6.2 Calculate the strain at 80% of the maximum stress, $\varepsilon_{0.8S_{Tmax}}$, as the ductility.

Note 14 – This parameter is calculated when 80% of the maximum tensile stress is reached after the ultimate applied load. Interpolate as necessary between data points.

$$\varepsilon_{0.8S_{Tmax}} = \frac{\delta}{t}$$

where:
δ = displacement at 80% after the ultimate applied load, in (or mm), and
t = thickness of specimen in (or mm).

7. REPORT

7.1 Report the following for each laboratory-molded specimen:

- asphalt binder type;
- test temperature;
- maximum stress, S_{Tmax};
- ductility, $\varepsilon_{0.8S_{Tmax}}$;
- additional comments.

8. PRECISION

8.1 The precision of this test method has not been established.

Standard Method of Test for

Poker Chip Test of Asphalt Binder

AASHTO Designation: X XXX-22[1]

Technical Subcommittee: 2b, Liquid Asphalt

Release: xxxx

AASHTO
American Association of State Highway and Transportation Officials
555 12th Street NW, Suite 1000
Washington, D.C. 20004

Standard Method of Test for

Poker Chip Test of Asphalt Binder

AASHTO Designation: X XXX-22[1]

Technical Subcommittee: 2b, Liquid Asphalt

Release: xxxx

AASHTO

1. SCOPE

1.1. This test method evaluates the tensile failure characteristics of an asphalt binder under a state of stress that induces high triaxiality in the asphalt binder, which models a realistic stress state similar to that exerted on asphalt binder confined between two aggregates. This test method is relevant for fatigue or thermal cracking in asphalt mixtures and can be used with material aged using T 240 (RTFOT) or R 28 (PAV), or both.

1.2. The values stated in SI units are to be regarded as the standard.

1.3. *This standard does not purport to address all of the safety concerns, if any, associated with its use. It is the responsibility of the user of this standard to establish appropriate safety and health practices and determine the applicability of regulatory limitations prior to use*.

2. REFERENCED DOCUMENTS

2.1. *AASHTO Standards*:

- M 320, Performance-Graded Asphalt Binder
- T 240, Effect of Heat and Air on a Moving Film of Asphalt Binder (Rolling Thin-Film Oven Test)
- R 28, Standard Practice for Accelerated Aging of Asphalt Binder Using a Pressurized Aging Vessel (PAV)

2.2. *ASTM Standard*:

- D8, Standard Terminology Relating to Materials for Roads and Pavements

3. TERMINOLOGY

3.1. *Definitions*

3.1.1. Definitions of terms used in this practice may be found in ASTM D8, determined from common English usage, or combinations of both.

3.2. *Definitions of Terms Specific to This Standard*:

3.2.1. *Tensile Strength* – the maximum tensile stress experienced by the sample during the test.

3.2.2. *Ductility* — the strain at 80% of the maximum stress, $\varepsilon_{(0.8S_{Tmax})}$, this parameter is calculated when 80% of the maximum tensile stress is reached after the maximum stress.

4. SUMMARY OF TEST METHOD

4.1. This test method is used to determine the tensile strength and ductility of an asphalt binder, under a load-controlled mode of loading. These parameters are related to the ability of an asphalt mixture to resist fatigue and thermal cracking. The specified temperature will typically be an intermediate temperature of 25 ± 0.5°C (77 ± 1°F), although other temperatures may be specified.

4.2. A sample of the RTFO-conditioned asphalt can be tested using the poker chip test. Also asphalt binder conditioned using both T 240 (RTFOT) and R 28 (PAV) can be tested. The poker chip geometry is used with a sample that is 1.5875 mm (0.0625 in) thick and 50.8 mm (2.0 in) in diameter. The sample is tested in tension under a monotonically increasing load. The load rate used is 2 N/s (0.25 lbf/s) until the sample fails.

5. SIGNIFICANCE AND USE

5.1. This method is designed to identify the tensile strength and ductility of an asphalt binder when subject to a monotonically increasing tensile load. Ductility of the asphalt binder has been shown to be an indicator of the asphalt mixture to resist fatigue and thermal cracking.

6. APPARATUS

6.1. *Testing Machine* — The testing machine or load frame, as shown in Fig. 6.1, should have the capability of applying tension in displacement- or load-controlled mode.

Note 1 — A servo hydraulic testing machine with a function generator capable of producing the desired displacement-controlled or load-controlled mode has been shown to be suitable for use in tension testing. Other commercially available electric motor actuators with at least 4 kN (900 lbf) load cell and frame can also be used.

Note 2 — The device should be capable of applying a displacement at a rate that can be as high as 150 mm/minute (5.9 in/minute).

6.1.1. The load frame must be set up to apply a seating load in displacement-controlled mode of 1 mm/minute (0.04 in/minute) until a tensile load of 40 N (9 lbf) is reached. At this point the load frame must be switched to load-controlled mode to apply a tensile load of 2 N/second (0.25 lbf/second) until the sample fails and during this time the load and displacement are recorded at a rate of at least 2 points per second.

6.1.2. The testing machine must be coupled with an automatic cut off system that can be programmed using a digital controller to stop the equipment in case of emergency.

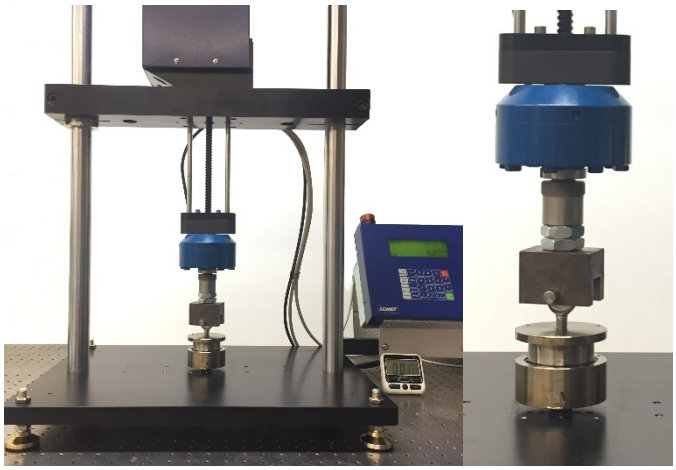

Figure 6.1 — Testing Machine (left: overall view of the load frame, right: closer view of the load cell)

6.2. *Measurement and Recording System* — The measurement and recording system should include sensors for measuring and recording vertical deformations and loads. The system should be capable of measuring vertical deformations with a resolution of at least 0.001 mm (0.00004 in) of deformation. Loads should be measured and recorded with a resolution of at least 0.1 N (0.0225 lbf).

6.2.1. The vertical deformation can be measured using a linear variable differential transducer (LVDT) or other suitable devices. The sensitivity and type of measurement device should be selected to provide the deformation readout required in 6.2.

6.2.2. The load should be measured with an electronic load cell capable of satisfying the specified requirements for load measurements in 6.2.

6.2.3. Refer to the manufacturer's specifications for system calibration and accuracy.

6.3. *Temperature-Controlled Chamber for Conditioning Specimen* — The temperature-controlled chamber should be capable of maintaining a temperature of 25°C (77°F), and within 0.5°C (1°F). The system should include a temperature-controlled chamber large enough to hold at least ten specimens for a period of at most 24 hours prior to testing.

6.4. *Heating Oven* — The oven must be capable of maintaining a temperature of 160 ± 3°C (320 ± 5°F).

6.5. *Stainless-Steel Mold* — The poker chip sample is prepared using a two-piece mold (top and bottom) and shall be similar in design to that shown in Figure 6.2 and 6.3. The mold shall be made of stainless steel, and dimensions of the assembled mold shall be as shown in Figure 6.2 and 6.3, with the permissible variations indicated. Two parts of the mold, as shown in Figure 6.4, are used to prepare a thin film specimen

Note 3 — The thread size and depth on the mold may vary based on the testing machine mounting system.

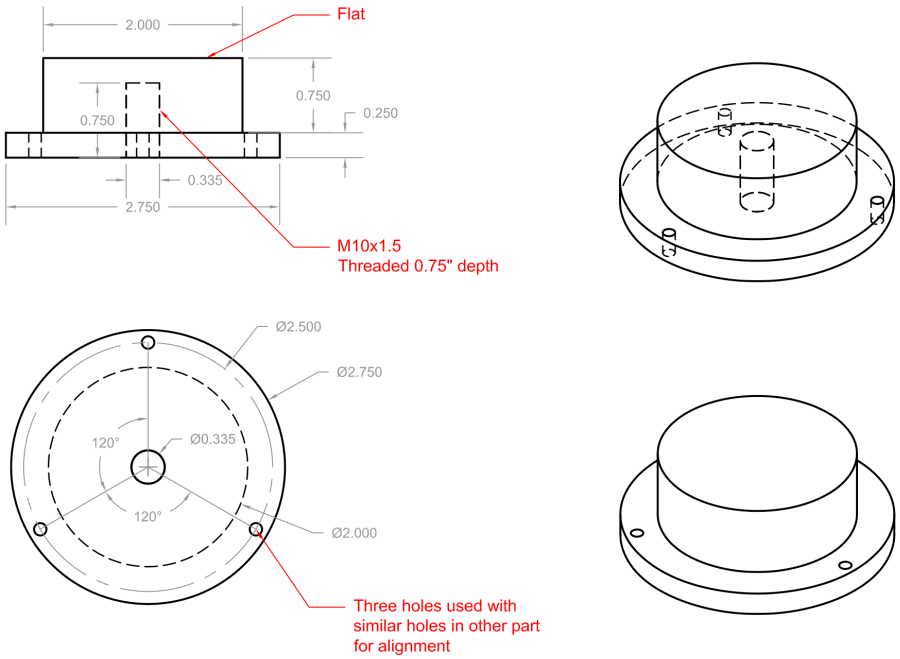

Figure 6.2 — Stainless-Steel Mold. Top piece of the poker chip mold (all dimensions in inches)

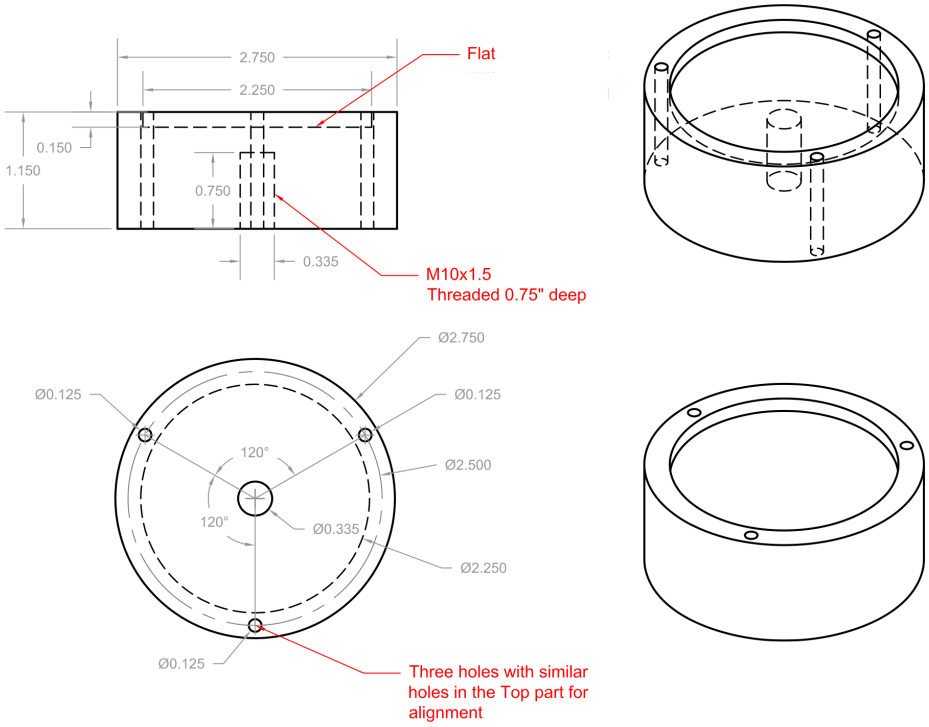

Figure 6.3 — Stainless-Steel Mold. Bottom piece of the poker chip mold (all dimensions in inches)

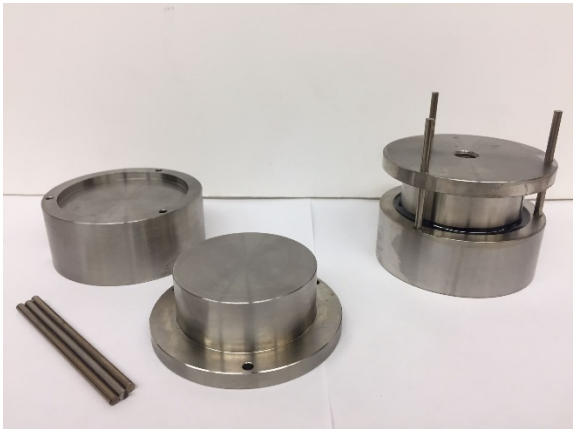

Figure 6.4 — Poker chip stainless-steel mold and laboratory-molded specimen between the top and bottom pieces that are aligned using three alignment pins (top and bottom of the mold with the three alignment rods are shown to the left and an assembled mold with the binder sample is shown to the right)

6.6. *Alignment pins* — The alignment pins are 3.1 ± 0.005 mm (0.122 ± 0.0002 in) in diameter and 69.85 mm (2 ¾ in) in length. The pins can be machined or purchased directly from a hardware supplier and shall be made of stainless steel. These alignment pins are run through the three holes in the top and bottom of the poker chip mold to ensure proper alignment of the two parts. Three alignment pins are needed for each poker chip mold.

6.7. *Spacer Dowels* — The spacer dowels are 0.0025 ± 1.18E-05 mm (1/16 ± 0.0003 in) in diameter and 0.005 mm (1/8 in) in length. The dowels can be machined or purchased directly from a hardware supplier and shall be made of alloy steel. These spacer dowels are dropped in the liquid asphalt binder to achieve the target thickness when placing the top part of the poker chip mold.

6.8. *Ball Joint Rod End* — The ball joint rod end can be machined or purchased directly from a hardware supplier and shall be made of alloy steel with a fully threaded bolt and a ball joint end type. This ball joint rod end is used on the top piece of the poker chip mold to connect to the load frame using an appropriate clevis pin and dowel.

6.9. *Silicone Molds* — The silicone molds are made of food grade silicone, bisphenol A (BPA) free, non-stick and flexible to easily release the asphalt binder from the molds. Typically, the temperature range of this material is from -40 to 241°C (-40 to 466°F). The diameter of each cavity is 25.4 mm (1.0 in) and the molds are 6.35 mm (1/4 in) deep. These dimensions hold approximately 4.5 g of asphalt binder properly.

6.10. *90 Degree Bent Nose Pliers* — A 90-degree bent nose plier is a variation of needle nose pliers. It features non-serrated tapered jaws that are bent at a 90-degree angle, 3/8" from the tip. This allows the jaws to grip the spacer dowels.

6.11. *Stainless Steel Trays* — Stainless steel trays with a size of 330 x 240 x 25 mm (13 x 9.5 x 1 in) and a flat rigid base can be used to carry multiple poker chip molds in and out of the oven.

6.12. *Acetone* — Acetone can be used to clean and remove dust from the surface of the stain-less steel and silicone molds.

6.13. *Dry wipes* — Dry paper tissue wipes provide an easy way to wipe up liquid and dust from the surface of the stainless steel and silicone molds.

6.14. *Balance* — Balance conforming to the requirements of AASHTO M 231, Class G2.

6.15. *Stainless Steel Micro Spatula* — The stainless steel spatula that is 22.5 cm (9.0 in) length and 5 x 0.78 cm (2 x 0.31 in) flat ends and mirror-like finish.

6.16. *Bubble Level* — The bubble level can be used to indicate whether the surface of the stainless steel trays containing the poker chip molds are horizontal (level) when placed in the oven or the temperature controlled chamber.

7. MATERIALS

7.1. *Asphalt Binder Specimen* — The asphalt binder can be aged using T 240 (RTFOT) or R 28 (PAV), or both.

7.2. *Recovered Specimen* — The recovered asphalt binder from asphalt mixture or reclaimed asphalt pavement (RAP) can be tested "as is" condition or it can be aged using R 28 (PAV).

8. SPECIMENS

8.1. *Laboratory-Molded Specimen* — Condition the asphalt binder in accordance with AASHTO T 240 (RTFOT). If long term aged asphalt binder is to be tested, obtain a test sample according to AASHTO R 28 (PAV). Two parts of the mold are used to prepare a thin film specimen of 50.8 mm (2.0 in) diameter with a 1.5875 mm (1/16 in) thickness. Note that the bottom part of the mold has a trough that is 57.15 mm (2.125 in) in diameter whereas the top part is 50.8 mm (2.0 in) in diameter, which is the surface area that is subjected to tension during the test.

Note 4 — The asphalt binder is heated inside a conventional oven until the material is sufficiently fluid. Typically, a temperature of 160 ± 3°C (320 ± 5°F) is adequate for most binders. Modified asphalt binders and RAP extracted binders may be heated to higher temperatures if material does not pour easily.

9. PROCEDURE

9.1. *Asphalt Binder Sample Preparation:*

9.1.1. Heat a 60 ml (2 oz) metal can containing the asphalt binder sample using an oven set to 160 ± 3°C (320 ± 5°F) for 15 to 20 minutes until the binder is fluid enough to be poured. These precautions will help avoid oxidative hardening and loss of volatiles that will further harden the sample. During the heating process, the sample should be covered.

9.1.2. Stir the sample thoroughly to ensure it is homogenous.

9.1.3. Pour 4.5 ± 0.05 g of the asphalt binder inside the silicon mold, as shown in Figure 9.1, label the mold and set it aside. Allow the silicon mold to cool to room temperature after pouring.

Note 6 — The same amount of asphalt binder sample can be poured directly into a clean pre-heated bottom part of the poker chip mold. However, the balance used must be insulated to protect the weighing plate from the pre-heated bottom part of the poker chip mold.

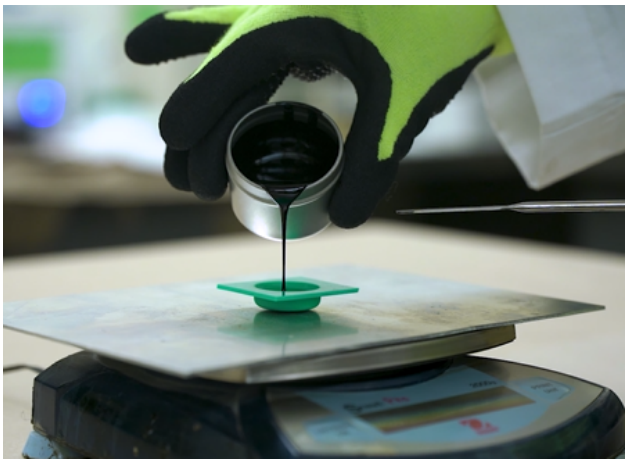

Figure 9.1 — Asphalt binder poured inside the silicone mold

9.2. *Laboratory-Molded Specimens Preparation:*

9.2.1. Wipe and clean the test faces of the poker chip mold (top and bottom) using Acetone.

9.2.2. Place the three alignment pins in the bottom part of the poker chip mold.

9.2.3. Preheat the top and bottom parts of the poker chip mold and the spacer dowels in an oven at 160 ± 3°C (320 ± 5°F) for at least 45 minutes. Poker chip molds can also be cleaned and left overnight in the oven.

Note 7 — Stainless steel trays can be used to handle multiple poker chip molds. Ensure that the oven trays are level using a bubble level prior to use.

9.2.4. Remove the pre-weighed dollop of the asphalt binder from the silicon mold and place it in the bottom part of the poker chip mold. Place the bottom part of the mold back in the oven at 160 ± 3°C (320 ± 5°F) for 15 minutes or until the dollop of asphalt binder has completely molten and spread over the entire bottom surface of the poker chip mold.

9.2.5. Place three spacer dowels approximately 120 degrees apart and about halfway radially out from the center of the bottom poker chip sample mold.

Note 8 — A 90 degree bent nose pliers can be used to grip the spacer dowels.

9.2.6. Place the bottom part of the poker chip mold back in the oven for another 5 minutes to allow the spacer dowels to sink and submerge in the binder.

Note 9 — The spacer dowels will be partially submerged due to the surface tension of asphalt binder.

9.2.7. Remove the bottom part and the pre-heated top part of the mold from the oven. Place two alignment pins in the lower part of the mold. Lower the top part of the poker chip mold slowly through the alignment pins and firmly press it at the center to ensure a correct set. Place the third alignment pin to ensure proper alignment.

Note 10 — Exercise caution. Plates are hot and the asphalt binder is fluid. Suddenly dropping the top part of the poker chip mold may cause the liquid binder to splash out.

9.2.8. Place the poker chip assembly in the oven at 160 ± 3°C (320 ± 5°F) for another 15 minutes.

9.2.9. Remove the poker chip assembly from the oven and let it cool to room temperature on a level platform.

Note 11 — If the asphalt binder spilled over to the lips of the mold, discontinue the procedure and discard the specimen.

9.2.10. Place the poker chip assembly inside a temperature-controlled chamber at 25 ± 0.5°C (77 ± 1°F). Ensure that the poker chip assembly is placed on a level platform using a bubble level.

Note 12 — If room temperature is within ± 0.5°C (± 1.0°F) of target temperature, the poker chip assembly can be cooled at room temperature.

9.3. *Mounting and Testing Laboratory Molded Specimens in the Testing Machine:*

9.3.1. Ensure that the load cell of the test machine is zeroed out with just the top part of the poker chip mold suspended from the loading axis.

9.3.2. Program the load frame to run the following sequence: i) apply tension in displacement-controlled mode at 1 mm/minute (0.04 in/minute) until a tensile load of 40 N (9 lbf) is reached, at this point ii) switch to load controlled mode and apply a tensile load of 2 N/second (0.25 lbf/second) until the sample fails.

9.3.3. Take the laboratory molded specimen and gently remove the alignment pins while holding the bottom of the specimen.
Note 13 — Do not use force to remove the alignment pins; if they appear stuck for any reason, gently tap using the back of a screwdriver and try to wiggle it free.

9.3.4. Check the lip of the bottom of the specimen to ensure that there is no binder that spilled over; this would indicate that the specimen was not cooled on a level platform and is not suitable for testing.

9.3.5. Lock the bottom of the poker chip assembly in the loading frame.

9.3.6. Thread in the ball joint rod on the top of the poker chip assembly and ensure it is finger tight but do not apply too much torque to avoid damaging the specimen.

9.3.7. Lower the loading axis gently until the clevis rod end hole aligns with the hole in the ball joint rod. Gently slide a dowel through the clevis rod end and the ball joint rod locking the two in place. Once the sample is locked in place, run the programmed test.

9.3.8. Start the test using the programmed sequence according to the section 9.3.2. The testing device automatically starts the test when the load frame has achieved a tensile load of 40 N (9 lbf). The displacement in the loading frame and corresponding strain in the specimen should be set to 0 at this seating load before the test begins.

9.3.9. Record the load and displacement at a rate of at least 2 points per second during all the test. Figure 9.1 shows a typical poker chip test output data.

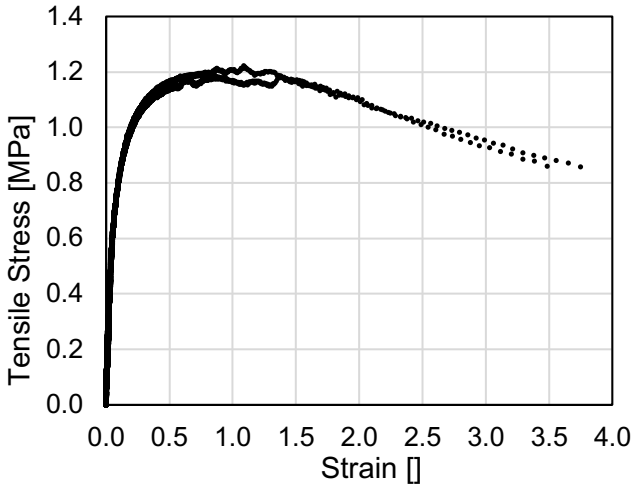

Figure 9.1 —Typical poker chip test output data

10. CALCULATIONS

10.1. Calculate the maximum stress, S_{Tmax}, recorded as the tensile strength as follows:

$$S_{Tmax} = \frac{4\,P_{ult}}{\pi D^2}$$

where:
P_{ult} = ultimate applied load required to fail specimen, N (or lbf), and
D = diameter of specimen, mm (or in).

10.2. Calculate the strain at 80% of the maximum stress, $\varepsilon_{0.8S_{Tmax}}$, and report this value as the ductility.
Note 14 — This parameter is calculated when 80% of the maximum tensile stress is reached after the ultimate applied load. Interpolate as necessary between data points.

$$\varepsilon_{0.8S_{Tmax}} = \frac{\delta}{t}$$

where:
δ = displacement at 80% after the ultimate applied load, in (or mm), and
t = thickness of specimen in (or mm).

11. REPORT

11.1. *Report the following information*:

11.1.1. Sample identification;

11.1.2. PG grade and test temperature, to the nearest 0.1°C;

11.1.3. Tensile strength, S_{Tmax}, *MPa*;

11.1.4. Ductility, $\varepsilon_{0.8S_{Tmax}}$, *%*; and

11.1.5. Additional comments.

12. PRECISION AND BIAS

12.1. *Precision* — The precision of this test method has not been established.

12.2. *Bias* — No information can be presented on the bias of the procedure because no material having an accepted reference value is available.

13. KEYWORDS

13.1. Asphalt binders; poker chip test, tensile strength, ductility, thermal cracking, fatigue cracking.